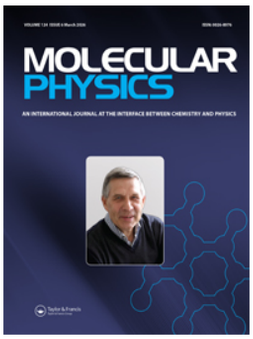

Taylor & Francis
Taylor & Francis Group

Molecular Physics

An International Journal at the Interface Between Chemistry and Physics

ISSN: 0026-8976 (Print) 1362-3028 (Online) Journal homepage: www.tandfonline.com/journals/tmph20

Surveying the ground electronic state potential energy surface of the 'mysterious' CO dimer

Marlene Bosquez, Piotr S. Żuchowski & Attila G. Császár

To cite this article: Marlene Bosquez, Piotr S. Żuchowski & Attila G. Császár (11 Mar 2026): Surveying the ground electronic state potential energy surface of the 'mysterious' CO dimer, Molecular Physics, DOI: 10.1080/00268976.2026.2628252

To link to this article: https://doi.org/10.1080/00268976.2026.2628252

MOLECULAR PHYSICS e2628252
https://doi.org/10.1080/00268976.2026.2628252

Taylor & Francis
Taylor & Francis Group

RESEARCH ARTICLE

OPEN ACCESS Check for updates

Surveying the ground electronic state potential energy surface of the 'mysterious' CO dimer

Marlene Bosquez[a,b], Piotr S. Żuchowski[c] and Attila G. Császár[a]

[a]Institute of Chemistry, ELTE Eötvös Loránd University, Budapest, Hungary; [b]ELTE Hevesy György PhD School of Chemistry, Budapest, Hungary; [c]Institute of Physics, Faculty of Physics, Astronomy and Informatics, Nicolaus Copernicus University in Toruń, Toruń, Poland

ABSTRACT

Eleven feasible stationary points have been located on the potential energy surface of the ground electronic state of $(CO)_2$ with shapes H, I , T, V, X, and Z. The global minimum has a planar, slipped, antiparallel arrangement of the atoms with a CC contact. There is a secondary minimum with an OO contact. The first-order transition state connecting the two minima has a CO contact. The remaining feasible stationary points are higher-order transition states. At intermediate levels of electronic structure theory, one can easily become lost in the web of polytopism. The relative energies of the most important stationary points were determined with the help of the focal-point analysis scheme. The relative energies are based on calculations up to the CCSDT(Q) level of electronic structure theory, basis sets up to aug-cc-pV6Z, and the inclusion of so-called 'small' corrections due to core-core and core-valence correlation, relativistic effects, and the diagonal Born–Oppenheimer correction. The electronic interaction energy of the global minimum is $-(hc)136.8(15)\ \mathrm{cm}^{-1}$, while the electronic energy difference between the global and local minima is $(hc)17.1(25)\ \mathrm{cm}^{-1}$. A detailed interaction energy analysis *via* symmetry-adapted perturbation theory suggests that the bonding in the dimer arises primarily from dispersion rather than electrostatics.

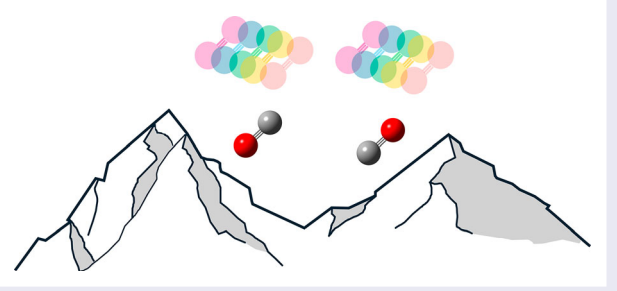

ARTICLE HISTORY
Received 8 December 2025
Accepted 28 January 2026

KEYWORDS
CO dimer; stationary points; focal-point analysis; symmetry-adapted perturbation theory (SAPT)

1. Introduction

Notable features of loosely bound van der Waals (vdW) complexes include not only the possibility of vanishing energy differences and small barrier heights between minima and other stationary points (SP) on their potential energy surfaces but also the exciting possibility that even the lowest vibrational and the rotational motions cannot be cleanly separated. Among the vdW complexes, the CO dimer stands out as a fascinating system, even called 'mysterious' by some high-resolution spectroscopists [1], that exhibits all the features mentioned. The structure, the bonding, the nuclear dynamics, and especially the (high-resolution) spectra of the CO dimer have intrigued the scientific community for decades [1–41].

As for the experimental spectroscopic studies on the CO dimer, the lack of clearly recognisable line patterns in the observed high-resolution spectra suggested [1, 32] that the CO dimer is a highly nonrigid species; thus, it might be considered a fluxional [42] or quasistructural [43] molecule, a supposition confirmed by sophisticated variational nuclear-motion computations [24, 29, 33]. Millimetre-wave (MMW) spectroscopists were able to identify rotational levels of both positive

CONTACT Attila G. Császár attila.csaszar@ttk.elte.hu Institute of Chemistry, ELTE Eötvös Loránd University, Pázmány Péter sétány 1/A, Budapest H-1117, Hungary

Supplemental data for this article can be accessed online at http://dx.doi.org/10.1080/00268976.2026.2628252.

and negative parity [1, 14, 25, 29]. It is an intriguing historical fact that these levels were first incorrectly interpreted as the splitting, due to tunnelling, of the vibrational ground state of a single $(CO)_2$ isomer [1, 25]. The correct picture arose from the analysis of band intensity patterns, which indicated the presence of two nearly isoenergetic forms of the CO dimer [21]. Further MMW measurements enabled the assignment of numerous rotational levels and the identification of several so-called 'stacks' of states [21]. Levels of a single isomer with different rovibrational quantum numbers and the same parity form the established stacks. Infrared (IR) spectroscopy yielded lines in the CO stretching fundamental region, between 2135 and 2155 cm^{-1} [1, 8, 11, 14, 16, 19, 44], and also provided evidence for the presence of two overlapping isomers: one was interpreted as a 'C-bonded' isomer, with an intermolecular bond distance of ≈4.4 Å, and the other as an 'O-bonded' isomer with a shorter intermolecular bond distance, ≈4.0 Å [19]. The isomer with a CC contact was found to be the lower-lying one, with an energy difference between the ground vibrational states of only 0.877 cm^{-1} [11]. The energy order of the isomers reverses when the CO stretch is excited by one quantum. The IR studies have been extended to isotopically substituted dimers as well, including the $^{13}C^{16}O$ [19, 27] and the $^{12}C^{18}O$ monomers [26]. These studies revealed that the ground states of the two isomers are separated by an energy difference that varies significantly with the isotopic composition, due to changes in the zero-point vibrational energies (ZPVE). While for the normal isotope, $^{12}C^{16}O$, the isomer with the CC contact, hereafter called Z_C, and the isomer with the OO contact, hereafter called Z_O, are separated by 0.877 cm^{-1} [14, 26], for the $^{13}C^{16}O$ and $^{12}C^{18}O$ dimers, the separations are found to be somewhat larger, 1.285 cm^{-1} [16], and smaller, 0.64 cm^{-1} [29], respectively. To properly account for these small differences, especially significant from a spectroscopic point of view, an accurate variational calculation of the zero-point vibrational energies is needed.

Computational searches [3, 9, 12, 15, 17, 18, 24, 28–30, 33] for the minima on the ground-electronic-state PES of the CO dimer have often produced qualitatively contradictory results, providing limited help to spectroscopists. In 1994, Havenith et al. [6] published the first set of experimental spectroscopic parameters for the CO dimer and hypothesised that a single non-planar structure of the dimer was consistent with their measurements. This claim was made despite the fact that earlier approximate calculations [3], using the multipole approximation and neglecting electron correlation in the exchange-repulsion energy, found a clear preference for planar structures. Then, in 1998, based on the analysis of a somewhat improved surface derived from that devised by van der Pol and co-workers [3], Meredith and Stone [9] located three minima and four first-order transition states, all planar except for one slightly non-planar TS. They loosely described the two lowest-energy planar minima as T-shaped, with either the C- or the O-end of a monomer pointing toward the other monomer (these shapes are called T_C and T_O in this study, respectively), and dismissed the slipped antiparallel structure found by van der Pol and co-workers [3] as a low-energy form of the dimer. In a 1999 study [12], van der Avoird and co-workers argued that higher-level variants of coupled cluster (CC) theory, namely CCSD(T) (that is CC theory with single, double, and a perturbative estimate of triple excitations) and CCSDT (CC theory with single, double, and triple excitations), still do not provide the correct asymptotic behaviour. Two further computational studies [17, 18] indicated that extended basis sets should be used to obtain an accurate potential energy surface (PES). Vissers et al. [24, 28] computed interaction PESs and suggested that there are two planar, slipped minima of shape Z and a first-order transition state of shape H connecting them. A decade later, Dawes et al. [33] selected the all-electron CCSD(T)-F12b level [45] without counterpoise correction [46] to determine a PES for the CO dimer. This PES owes its apparent accuracy to the compensation for basis set superposition error and the neglect of post-CCSD(T) electron correlation effects. The global and local minima on this PES correspond to shapes Z_C and Z_O, respectively. Finally, it should also be noted that the description of the interactions of molecules with triple bonds is known to be particularly difficult [47].

The weakly bound $(CO)_2$ dimer provides a nice opportunity to address the use of two schemes designed to improve basis set convergence toward the complete basis set limit. The first is the Boys–Bernardi (counterpoise, CP) correction [46], which corrects for the basis set superposition error on the relative energies and structures of vdW complexes. Recall that for H-bonded systems, the effects of the CP correction on the structures, the gradients (first geometric derivatives), and the Hessians (second geometric derivatives) have been investigated in considerable detail [48–50]. The second is the use of explicitly correlated techniques of electronic structure theory; these R12 [51, 52] and F12 [45, 53–56] techniques significantly improve basis set convergence toward the complete basis set (CBS) limit [57, 58].

To summarise the previous computational studies on $(CO)_2$, they revealed that (a) the ground-state electronic structure does not require a multi-reference treatment, single-reference techniques should be sufficient to obtain accurate results; (b) electron correlation beyond CCSD

[59] is important; (c) large basis sets need to be used to obtain reliable results; and (d) core-core and core-valence correlation effects may not be neglected. The difficulties and challenges mentioned motivated us to survey, based on the highest feasible levels of electronic structure theory, the stationary points of the ground electronic state PES of the CO dimer. The most important characteristics of the present study are as follows: (a) it systematically explores the stationary points on the ground electronic state PES of the CO dimer, identifying possible minima and transition states of different orders that govern nuclear motions; (b) based on the focal-point analysis (FPA) technique [60, 61], it provides estimates for the interaction energies and the relative energies of the stationary points with conservative uncertainty estimates; (c) it investigates the advantages of using the counter-poise correction scheme and explicitly correlated (F12) techniques [45, 53–56] for this challenging and somewhat pathological case; and (d) several levels of symmetry-adapted perturbation theory (SAPT) [62, 63] are used to deepen our understanding of the origin, strength, and directionality of the bonding in the CO dimer and the energy order of the stationary points through energy decomposition.

2. Methodological details

Stationary points on the ground-state PES of the CO dimer have been searched for and identified at several correlated levels of electronic structure theory, with particular emphasis on the second-order Møller–Plesset (MP2) [64] and CCSD(T) [65] levels. The interaction energy of the CO dimer is small, and the PES is flat along the intermonomer nuclear degrees of freedom. For these reasons, and to avoid the 'non-zero force dilemma' [66, 67], unusually tight convergence criteria had to be applied during the geometry optimizations and the computation of the nuclear first and second derivatives. This created a problem, especially for transition states with lower point-group symmetry, whose energy is close to that of other SPs or the first dissociation limit of the dimer. Our extensive computations confirmed that the CO dimer is a case where one can wonder in the web of polytopism [68], while small changes in the methods and basis sets are made.

The geometry optimizations were performed at the single-reference MP2 [64], MP2-F12 [53], CCSD(T) [65], and CCSD(T)-F12b [45] levels of electronic structure theory. The T_1 diagnostic values [69] of coupled-cluster theory are between 0.015 and 0.020 for the stationary points investigated; thus, single-reference techniques are adequate for studying the electronic structure of the CO dimer across large regions of the PES.

The basis sets used in the electronic structure computations of this study are restricted to the correlation-consistent aug-cc-p(C)VXZ family of Dunning [70], with $X = 2$(D), 3(T), 4(Q), 5, and 6. The aug-cc-pVXZ basis sets, abbreviated here as aXZ, have only been used for frozen-core (FC) calculations, keeping the 1s orbitals of C and O frozen, which leads to the correlation of the 10 valence electrons of each monomer unit. To estimate the core-core and core-valence correlation effects, the basis sets aug-cc-pCVXZ, with $X = 2$(D), 3(T), 4(Q), and 5, abbreviated as aCVXZ, have been used in each all-electron computation.

Correction for the basis set superposition error (BSSE), especially for the smaller atom-centred, fixed-exponent Gaussian basis sets, was achieved in this study through the use of the Boys–Bernardi [46] counterpoise correction scheme. The CP-corrected energy, E_{AB}^{CP}, for the dimer AB composed of fragments A and B, is given by the simple five-term expression

$$E_{AB}^{\mathrm{CP}} = E_{AB}^{\mathrm{AB}} - \left[\left(E_{A}^{\mathrm{AB}} - E_{A}^{\mathrm{A}}\right) + \left(E_{B}^{\mathrm{AB}} - E_{B}^{\mathrm{B}}\right)\right], \quad (1)$$

where E_{AB}^{AB} is the energy of the full AB dimer in the full AB basis set, E_{A}^{AB} is the energy of fragment A in the full (AB) basis (with fragment B as 'ghost'), E_{A}^{A} is the energy of fragment A in its own basis set, and analogously for E_{B}^{AB} and E_{B}^{B}.

The FPA [60, 61] energy estimates were obtained at structures fully optimised at the frozen-core, counterpoise-corrected aug-cc-pVQZ CCSD(T) level. The FPA analyses of the present study involve both CP-corrected and CP-uncorrected interaction energies. Extrapolation to the CBS limit was performed separately for the Hartree–Fock energies [71] and the electron correlation contributions [57, 72, 73] *via* the formulas

$$\Delta E_{\mathrm{int}}^{\mathrm{HF}[X,X+1]} = \Delta E_{\mathrm{int}}^{\mathrm{HF},X} + \frac{\Delta E_{\mathrm{int}}^{\mathrm{HF},X+1} - \Delta E_{\mathrm{int}}^{\mathrm{HF},X}}{1 - (1 + \frac{1}{X+1}) \exp\left\{9\left(\sqrt{X} - \sqrt{X+1}\right)\right\}} \quad (2)$$

and

$$\delta E_{\mathrm{int}}^{\mathrm{corr}[X,X+1]} = \delta E_{\mathrm{int}}^{\mathrm{corr},X} + \frac{\delta E_{\mathrm{int}}^{\mathrm{corr},X+1} - \delta E_{\mathrm{int}}^{\mathrm{corr},X}}{1 - \left(\frac{X}{X+1}\right)^3}, \quad (3)$$

respectively.

The FPA analyses involve three so-called 'small correction terms' [60, 61], which were considered for selected SPs. First, core-core and core-valence electron correlation were estimated by conducting all-electron and frozen-core computations using the aug-cc-pCVXZ basis sets. Second, scalar relativistic corrections have

been computed at the one-electron mass-velocity and Darwin (MVD1) level [74, 75] using the all-electron aug-cc-pCVTZ and aug-cc-pCVQZ CCSD(T) wave functions. Knowing the extremely slow convergence of the MVD1 correction with respect to the basis set size [75], no attempt was made to obtain these energy corrections using even larger basis sets. Third, diagonal Born–Oppenheimer (DBOC) [76, 77] energy corrections were computed at the restricted Hartree–Fock (RHF), MP2, and CCSD levels. No geometry optimizations were performed that considered the relativistic or DBOC corrections.

For weakly bound vdW complexes, such as $(CO)_2$, the zero-point vibrational energy cannot be estimated with sufficient accuracy using the harmonic-oscillator approximation. Nevertheless, to check whether the SPs determined are minima or transition states of different orders, second-derivative computations have been performed. Most SPs turned out to be transition states. In this study, TS*n* refers to a *n*th-order transition state (TS0, with a Hessian index of zero, is a minimum).

In the SAPT approach [62], the total Hamiltonian of the dimer *AB* is separated into the Hamiltonians of the isolated monomers *A* and *B* and the intermolecular interaction operator,

$$\hat{H}_{AB} = \hat{H}_A + \hat{H}_B + \lambda \hat{V}. \tag{4}$$

This choice defines an expansion of the interaction energy in a power series in $\hat{V}$. An essential element of SAPT is symmetry enforcement, whereby, to account for Pauli (exchange) repulsion, the antisymmetrizer for all electrons in the system is applied to the product of monomer wave functions in the energy expressions. For many-electron systems, SAPT cannot be used with the exact monomer wave functions; thus, approximations are necessary. In the present paper, three variants of SAPT are used for the analysis of interaction energies. In SAPT0, the intramonomer correlation is completely neglected, corresponding to the case where the monomers are described at the Hartree–Fock level. In the SAPT2+3(CCD) approximation, as denoted in the `PSI4` code [78] and described in Refs. [79, 80], one includes full third-order SAPT for intramonomer correlation in the first order in *V* (electrostatics and exchange) [81], while dispersion is given in the CCD approximation, as introduced by Williams et al. [82]. Finally, we use SAPT(DFT) [83–85] based on gradient-regulated asymptotic corrections with the PBE0 functional [86], which was recommended for use with SAPT [84, 87].

The electronic structure codes, in alphabetical order, `CFOUR` [88], `Gaussian16` [89], `MOLPRO` [90], `MRCC` [91, 92], and `PSI4` [78] have been utilised during this study. The counterpoise-corrected MP2 computations were performed with the codes `Gaussian16` and `MOLPRO` (when checked, they provided the same answer; most of the time, the latter code used numerical first- and second-derivative information). The counterpoise-corrected geometry optimizations at the CCSD(T) level used the `MOLPRO` package [90] and numerically computed counterpoise-corrected gradients [48, 49]. `MOLPRO` has been used for all the explicitly correlated F12 computations (the MP2-F12 energies used in this study are referred to as MP2-F12/3C(F) in the code). The XSURF package of `MOLPRO` [93, 94] was used for some of the second-derivative tests. `MRCC` has been used for the highest-level coupled-cluster computations. The package `PSI4` was used for the different SAPT calculations.

3. Results and discussion

The electronic-structure computations yielded a substantial amount of data. Geometry optimizations, followed by second-derivative tests, were performed at the MP2, MP2-F12, CCSD(T), and CCSD(T)-F12b levels for 12 shapes on the ground-electronic-state PES of $(CO)_2$. No stationary point was found for the shape V_C, with an equilibrium structure of C_{2v} point-group symmetry; however, all other stationary points were found at several levels of electronic structure theory, often with different Hessian indices. For the remaining 11 stationary points, Tables 1–3 include, at each level of theory considered, the electronic energies of the stationary points, E_{el}, and the corresponding interaction energy estimates, ΔE_{int}, which are the differences between the energy of the stationary point and the two non-interacting monomers, as well as the outcomes of the second-derivative tests, whenever available, that determine the Hessian index *n* of the stationary points, listed as TS*n*. These results are reported both for calculations that did not consider the counterpoise correction ('no CP') and for those in which the counterpoise correction was considered ('wCP'). In a few cases, we observed clear convergence issues, especially during the numerical second-derivative calculations. These are noted in Tables 1–3. It is possible that subtle numerical problems may have resulted in incorrect Hessian indices. Structural parameters of the reference geometries chosen for the focal-point analysis (FPA) of the electronic interaction energies characterising the stationary points on the ground electronic state potential energy surface of $(^{12}C^{16}O)_2$ are given in Table 4; these structural parameters are highly similar to those obtained at other levels of theory. Accurate interaction energies and conservative uncertainty estimates for specific SPs, obtained using the FPA scheme [60, 61], are

provided in Tables 5 and 6 for some of the stationary points. Table 7 lists interaction energy components obtained at various levels of SAPT approximations; they help to understand the bonding characteristics of the CO dimer. The two tables of the Supplementary Material provide additional data supporting the FPA and SAPT analyses.

3.1. Stationary points

To the best of our knowledge, no computational studies, perhaps with the exception of those by Meredith and Stone [9], have systematically surveyed stationary points other than minima on the ground electronic state potential energy surface of the CO dimer. The present computations were carried out not only to fill this gap but also to aid in determining the appropriate level of electronic-structure theory required for an accurate description of the full-dimensional PES, which is planned to be conducted in the future, upon which detailed nuclear motion computations [95] can be performed to better understand the dynamics and the 'mysterious' spectroscopy of isotopologues of the CO dimer.

The previous computational studies [3, 9, 12, 15, 17, 18, 24, 28–30, 33] on the ground electronic state PES of the CO dimer have usually identified two isomers with similar energies; however, these isomers differed in their shapes and relative energies. In recent years [33], it has been widely accepted, based on CCSD(T)-type computations that occasionally correlated all the electrons, that both isomers have a planar, slipped, antiparallel arrangement of the atoms, which is referred to in this study as shape Z (see the figures in Table 1). Some of the earlier studies [3] have found T-shaped minima, referred to here as T_C and T_O (see the related figures in Table 2). As for experimental studies yielding structural estimates, Brooks and McKellar [11] supported the concept that two isomers co-exist in their measurements with almost the same relative energies, whereby T_C was assumed to be the 'true global minimum'. The difficulties associated with locating minima on the PES of the CO dimer have been acknowledged for decades; see, for example, Figure 1 of Ref. [3]. The most important statements related to this figure are as follows: (a) the shape I_C is not a minimum (confirmed in this study; in fact, at higher levels of theory, this stationary point does not even exist); (b) the T_C form may correspond to a very shallow minimum; and (c) while several possible shapes have been considered, the stable, slipped, antiparallel Z-shaped forms were not even considered due to the relatively low levels of electronic structure theory used.

The simplest way to find stationary points is through geometry optimizations aimed at finding minimum-energy structures. These straightforward energy minimizations along the geometric degrees of freedom might not yield minima but rather transition states of different orders once (a) appropriate symmetry constraints are in place and (b) changing the initial point-group symmetry is not permitted. This is how the linear structures, the supposedly fourth-order transition states I_O, I_C, and I_M, have been optimised in this study (see Table 3). Transition states can also be searched for using specialised algorithms, such as versions of eigenvector-following techniques [96, 97]. Exploration of minima and first-order transition states, as well as the connecting pathways, is built into several electronic structure packages. In the fourth column of Tables 1–3, searches for minima and transition states are denoted by the letters 'M' and 'T', respectively.

Systematic geometry optimizations, searching for minima and transition states in the chosen subspace, yielded stationary points corresponding to several feasible shapes of the CO dimer. The starting point was our computational study of the N_2 dimer [73], whereby stationary points with shapes Z, H, T, X, and I were obtained. In this study, the shape V was added to this list. Compared to the N_2 dimer, an important feature of the CO dimer is that one loses the equivalence of the two atoms within the two monomer units of the dimer, which usually doubles or even triples the number of feasible initial structures. This fact is reflected in the naming convention applied in this study: for each shape, we need to distinguish at least two cases, depending on which atoms of the monomers are in closest contact. This means, for example, that there are two highly symmetric Z-shaped forms, namely Z_C and Z_O (see the graphical images in Table 1). These names are formal and do not reflect the bonding situation in the dimer: Z_C is more favoured than Z_O due not simply to the more favourable arrangement of the two small dipoles of the monomers, as they are antiparallel in both Z_C and Z_O, but to subtle interaction effects (see Section 3.4 below). Furthermore, there is a third Z-shaped structure, Z_M (subscript M means mixed), when the C and O atoms of the two monomers, with opposite partial charges, happen to be close to each other (note that the form Z_M appears only when attempting to locate a transition state). Similarly, there are three possible linear (I-shaped) arrangements of the two CO monomers: two of which have $D_{\infty h}$ point-group symmetries (either the two oxygen atoms, in the case of I_O, or the two carbon atoms, in the case of I_C, are in contact) and one, I_M, with an equilibrium structure of $C_{\infty v}$ point-group symmetry, when the partial charges are aligned in a favourable fashion.

Table 1. Results of geometry optimizations yielding stationary points of shape Z[a].

Stationary point(symm.)	Level of theory	Basis	M/T	$E_{el}^{no\ CP}/E_h$	$\Delta E_{int}^{no\ CP}/cm^{-1}$	TS*n*(symm.)	E_{el}^{wCP}/E_h	$\Delta E_{int}^{w\ CP}/cm^{-1}$	TS*n*
Z-shaped, $Z_C(C_{2h})$	MP2	aDZ	M	−226.110 969	−225.9	1(B_u)	−226.110 538	−131.3	0
		aCVDZ	M	−226.265 864	−245.2	1(B_u)	−226.265 351	−132.6	0
		aTZ	M	−226.285 684	−189.2	0	−226.285 469	−141.9	0
		aCVTZ	M	−226.494 701	−184.8	0	−226.494 511	−143.1	0
		aQZ	M	−226.346 642	−174.9	0	−226.346 527	−149.5	0
		aCVQZ	M	−226.570 622	−171.7	0	−226.570 529	−151.3	0
		a5Z	M	−226.368 641	−161.6	0	−226.368 602	−152.6	0
		aCV5Z	M	−226.596 481	−162.1	0	−226.596 448	−154.8	0
		a6Z	M	−226.377 459	−163.6	0	−226.377 438	−158.9	0
	MP2-F12	aDZ	M	−226.362 800	−164.1	0	−226.362 739	−150.6	0
		aTZ	M	−226.374 528	−160.5	2	−226.374 499	−154.1	0
		aQZ	M	−226.385 271	−158.7	0	−226.385 258	−155.8	0
		a5Z	M	−226.388 353	−157.7	0	−226.388 336	−154.0	
	CCSD(T)	aDZ	M	−226.149 047	−206.6	1(B_u)	−226.148 590	−106.4	1
		aCVDZ	M	−226.309 957	−225.9	1(B_u)	−226.309 418	−107.6	1
		aTZ	M	−226.325 138	−164.8	1(B_u)	−226.324 931	−119.4	1
		aCVTZ	M	−226.540 990	−159.6	1(B_u)	−226.540 811	−120.3	1
		aQZ	M	−226.381 418	−148.3	0	−226.381 321	−126.9	1
		aCVQZ	M	−226.611 997	−145.5	0	−226.611 918	−128.2	
		a5Z	M	−226.399 173	−136.0	1(B_u)	−226.399 148	−130.4	
		aCV5Z	M	−226.633 450	−135.8		−226.633 426	−130.6	
		a6Z	M	−226.405 381	−133.7	—[b]	−226.405 373	−131.7	
	CCSD(T)-F12b	aDZ	M	−226.358 209	−142.9	1	−226.358 097	−118.3	1
		aTZ	M	−226.386 456	−142.0	1	−226.386 389	−127.3	1
		aQZ	M	−226.404 080	−137.9	1	−226.404 049	−131.0	1
		a5Z	M	−226.409 506	−134.4				
Z-shaped, $Z_O(C_{2h})$	MP2	aDZ	M	N/A($Z_O \rightarrow I_O$)	–	–	−226.110 460	−114.2	0
		aCVDZ	M	N/A($Z_O \rightarrow I_O$)	–	–	−226.265 269	−114.6	0
		aTZ	M	−226.285 637	−178.8	0	−226.285 403	−127.6	0
		aCVTZ	M	−226.494 640	−171.6	0	−226.494 440	−127.5	0
		aQZ	M	−226.346 552	−154.9	0	−226.346 443	−130.8	0
		aCVQZ	M	−226.570 527	−150.8	0	−226.570 439	−131.6	0
		a5Z	M	−226.368 564	−144.2	0	−226.368 518	−134.7	0
		aCV5Z	M	−226.596 395	−143.1	0	−226.596 356	−134.5	
		a6Z	M	−226.377 378	−145.8	1(A_u)	−226.		
	MP2-F12	aDZ	M	−226.362 754	−154.0	0	−226.362 680	−137.8	0
		aTZ	M	−226.374 462	−146.0	0	−226.374 434	−139.9	0
		aQZ	M	−226.385 183	−139.3	0	−226.385 172	−136.9	0
		a5Z	M	−226.388 268	−139.0	1	−226.388 259	−137.1	—[b]
	CCSD(T)	aDZ	M	−226.148 926	−180.1	1(B_u)	−226.148 533	−93.7	1
		aCVDZ	M	−226.309 792	−189.7	1(B_u)	−226.309 352	−93.1	1
		aTZ	M	−226.325 141	−165.4	0	−226.324 901	−112.8	1
		aCVTZ	M	−226.540 930	−146.4	1(B_u)	−226.540 774	−112.2	1
		aQZ	M	−226.381 379	−139.8	1(B_u)	−226.381 279	−117.9	1
		aCVQZ	M	−226.611 934	−131.7	1(B_u)	−226.611 867	−116.9	1
		a5Z	M	−226.399 135	−127.7	0	−226.399 104	−120,9	
		aCV5Z	M	−226.633 398	−124.3		—		
		a6Z	M	−226.405 341	−124.8		—		
	CCSD(T)-F12b	aDZ	M	−226.358 158	−131.7	1	−226.358 050	−108.0	1
		aTZ	M	−226.386 416	−133.1	0	−226.386 364	−121.9	1
		aQZ	M	−226.404 034	−127.8	1	−226.404 009	−122.2	
		a5Z	M	−226.409 466	−125.7		−226.409 455	−123.2	
Z-shaped, $Z_M(C_s)$	MP2	aDZ	T	−226.110 691	−164.7	1(A')	−226.110 347	−89.2	1
		aCVDZ	T	−226.265 552	−176.8	1(A')	−226.265 154	−89.5	1
		aTZ	T	−226.285 472	−142.6	1(A')	−226.285 286	−101.8	1
		aCVTZ	T	−226.494 492	−138.9	1(A')	−226.494 327	−102.8	1
		aQZ	T	−226.346 430	−128.4	1(A')	−226.346 334	−107.3	1
		aCVQZ	T	−226.570 412	−125.6	1(A')	−226.570 332	−108.0	
		a5Z	T	−226.368 446	−118.7	1(A')	−226.368 408	−110.4	
		aCV5Z	T	−226.596 279	−117.7		−226.596 248	−110.9	
		a6Z	T	−226.377 262	−120.4		—		
	MP2-F12	aDZ	T	−226.362 594	−118.9	1	−226.362 538	−106.7	1
		aTZ	T	−226.374 333	−117.7	1	−226.374 306	−111.9	1
		aQZ	T	−226.385 073	−115.2	1	−226.385 063	−112.9	1

(*continued*).

Table 1. Continued.

Stationary point(symm.)	Level of theory	Basis	M/T	$E_{el}^{no\,CP}/E_h$	$\Delta E_{int}^{no\,CP}/cm^{-1}$	TS*n*(symm.)	E_{el}^{wCP}/E_h	$\Delta E_{int}^{w\,CP}/cm^{-1}$	TS*n*
		a5Z	T	−226.388 156	−114.5				
	CCSD(T)	aDZ	T	−226.148 912	−177.0	1(*A′*)	−226.148 550	−97.5	1
		aCVDZ	T	−226.309 792	−189.7	1(*A′*)	−226.309 366	−96.3	1
		aTZ	T	−226.325 075	−150.9	1(*A′*)	−226.324 884	−109.1	1
		aCVTZ	T	−226.540 927	−145.6	1(*A′*)	−226.540 760	−109.1	1
		aQZ	T	−226.381 361	−135.9		−226.381 263	−114.4	1
		aCVQZ	T	−226.611 927	−130.2		–		
	CCSD(T)-F12b	aDZ	T	−226.358 144	−128.6	1	−226.358 041	−106.0	1
		aTZ	T	−226.386 396	−128.8	1	−226.386 335	−115.6	1
		aQZ	T	−226.404 029	−126.7		−226.404 004	−121.2	
		a5Z	T	−226.409 446	−121.1		–		

Note: [a] All geometry optimizations with the aug-cc-pV*X*Z ('a*X*Z') basis sets [70], X = 2(D), 3(T), 4(Q), 5, and 6, were performed within the frozen-core approximation, while in the case of the aug-cc-pCV*X*Z ('aCV*X*Z') basis sets, X = 2(D), 3(T), 4(Q), 5, all of the electrons were correlated. MP2 = second-order Møller–Plesset perturbation theory, CCSD(T) = coupled cluster theory with singles, doubles, and perturbative estimates of triples. Basis = atom-centred, fixed-exponent, Dunning-type [70] Gaussian basis sets. CP = counterpoise correction [46]. $E_{el}^{no\,CP}$ and $\Delta E_{int}^{w\,CP}$ are the computed total energies without and with CP, respectively. Similarly, ΔE_{int}^{noCP} and ΔE_{int}^{wCP} are the relative interaction energies without and with CP, respectively, computed with respect to the total energies of two CO monomers at the given level of theory. TSn = nth order transition state (where the n = 0 value of the Hessian index indicates a minimum). For first-order TSs the symmetry of the imaginary mode is given in parentheses. N/A = The stationary point corresponding to this shape could not be located. M/T = Searching for a minimum (M) or a transition state (T). [b] Numerical stability issues.

High-energy stationary points on the [C,C,O,O] PES, such as the linear arrangement O=C=C=O, a covalent dimer of carbon monoxide [98–100], also called ethylenedione, were not considered in our final analysis, although geometry optimizations were performed for them. Therefore, we can note that O=C=C=O is a first-order transition state (TS1) at the frozen-core MP2 level, with all the basis sets aug-cc-pV*X*Z, X = D, T, Q, and a relative energy that is much larger than the first dissociation limit of the vdW CO dimer.

It should also be mentioned that, at certain levels of electronic-structure theory, further curious high-energy stationary points have been located on the CO dimer PES. For example, for the I_O shape, in frozen-core optimizations without CP correction, one can obtain stationary points other than the one presented in Table 3. In these spurious stationary points, either the monomer CO bond length or the intermonomer OO distance becomes significantly longer, resulting in high relative energies. Even more curiously, these SPs can be minima at that level of theory. These results emphasise the difficulties that lower levels of theory have in properly describing the electronic structure of even the ground electronic state of the CO dimer. Further difficulties are expected for the excited electronic states of the CO dimer, where the highly stable carbon dioxide plus a carbon atom and an O=C=C=O structure may become competitive in energy with true vdW-dimer-like shapes.

At all the electronic structure theory levels used in this study, the shape Z_C is a minimum. Nevertheless, the shape Z_C with point-group symmetry C_{2h}, $Z_C(C_{2h})$, which has been considered the global minimum in a number of recent studies, is *not* a minimum when the aug-cc-pVDZ basis set is used, either at the traditional MP2 or CCSD(T) levels. Somewhat more disturbingly, at the traditional frozen-core aug-cc-pV*X*Z CCSD(T) levels, $Z_C(C_{2h})$ is a minimum only for X = Q. The inclusion of core correlation does not change the situation. The use of the counterpoise correction clearly changes the stability situation at the MP2 level, as all the MP2 optimizations yield minima for $Z_C(C_{2h})$ when the CP correction is included. This observation also highlights how careful one must be with the results obtained at intermediate levels of electronic-structure theory for the CO dimer. When the Z_C and T_C entries of Tables 1 and 2, respectively, are compared, it is clear that when the $Z_C(C_{2h})$ structure is a transition state, a slightly distorted structure, called T_C, is a minimum with essentially the same relative energy. This minimum-energy structure could as well be called $Z_C(C_s)$, as the structure is much closer to a Z shape than to a T shape. In summary, based on all geometry optimizations, Z_C is clearly the shape of the global minimum on the ground electronic state PES of the CO dimer, though the point-group symmetry of the equilibrium structure, C_{2h} *vs.* C_s, remains unclear.

Similar comments apply to the Z_O isomer as they do to the Z_C one; the shape $Z_O(C_{2h})$ is a minimum in only about half of the cases (see Table 1). There is a drastic difference, though: when the $Z_O(C_{2h})$ transition state structure is relaxed and the point group is C_s, the optimised structure is better described as having the shape T_O rather than Z_O. Based on the experimental spectroscopic findings, one must choose T_O (or Z_O) as a low-energy isomer of the CO dimer.

We searched for the first-order transition state connecting the two minima. It was found that the shape Z_M, where the shortest intermonomer distance is between an O and a C atom, is a transition state at all levels of theory, and it has C_s point-group symmetry. It proved to be straightforward to locate this transition state (see the

Table 2. Results of geometry optimizations yielding stationary points of shape X, H, T, and V[a].

Stationary point (symm.)	Level of theory	Basis	M/T	$E_{el}^{no\,CP}/E_h$	$\Delta E_{int}^{no\,CP}/cm^{-1}$	TS*n*(symm.)	E_{el}^{wCP}/E_h	$\Delta E_{int}^{w\,CP}/cm^{-1}$	TS*n*
X-shaped, X(C_2)	MP2	aDZ	T	−226.110 646	−155.0	1(*A*)	−226.110 278	−74.2	2(*A*, *B*)
			T	−226.110603	−145.6	2(*A*, *B*)			
		aCVDZ	T	−226.265 487	−162.5	1(*A*)	−226.265 086	−74.5	2(*A*, *B*)
		aTZ	T	−226.285 400	−126.6	2(*A*, *B*)	−226.285 207	−84.4	
		aCVTZ	T	−226.494 423	−123.8	2(*A*, *B*)	−226.494 269	−90.0	
	MP2-F12	aDZ	T	−226.362 720	−146.5		−226.362465		−90.6 1
		aTZ	T	N/A(X→ Z_O)	–		−226.374244		−98.2 1
		aQZ	T	−226.385 157	−133.6				
		a5Z	M	N/A(X→ Z_O)	–				
	CCSD(T)	aDZ	T	−226.148 722	−135.3	1(*A*)	−226.148 550	−97.7	
		aCVDZ	T	−226.309 602	−148.0	1(*A*)	−226.309 602	−148.1	
		aTZ	T	−226.324 882	−108.6	2(*A*, *B*)	−226.324 901	−112.7	
		aCVTZ	T	−226.540 737	−104.1	2(*A*, *B*)	−226.540 737	−104.0	
		aQZ	T	−226.381 110	−80.8	2(*A*, *A*)	−226.381 182	−96.6	
		aCVQZ	T	−226.611 694	−79.0				
	CCSD(T)-F12b	aDZ	M	N/A(X→ Z_O)	–				
			T	−226.357 889	−72.7				
		aTZ	M	N/A(X→ Z_O)	–				
			T	−226.386 135	−71.6				
		aQZ	T	−226.403 862	−90.0				
		a5Z	M	−226.409 452					
H-shaped, H_M(C_{2h})	MP2	aDZ	T	−226.110 289	−76.6	2(A_g, A_u)	−226.109 990	−11.0	2
		aCVDZ	T	−226.265 151	−88.8	2(A_g, A_u)	−226.264 800	−11.7	2
		aTZ	T	−226.285 083	−57.3	2(A_g, A_u)			
		aCVTZ	T	−226.494 113	−55.8	2(A_g, A_u)			
		aQZ	T	−226.346 067	−48.7	2(B_g, A_u)			
		aCVQZ	T	−226.570 057	−47.6				
		a5Z	T	−226.368 099	−42.6				
		aCV5Z	T	−226.595 936	−42.5				
	MP2-F12	aDZ	M				N/A(H_M→ Z_C)		
		aDZ	T	−226.362 244	−42.1	2	−226.362 194	−31.2	2
		aTZ	T	−226.373 981	−40.5	2	−226.373 963	−36.4	2
		aQZ	T	−226.384 729	−39.6		−226.384 721	−37.8	2
		a5Z	T	−226.387 814	−39.4				
	CCSD(T)	aDZ	T	−226.148 655	−120.4	2(A_g, A_u)	N/A(H_M→ Z_O)		
		aCVDZ	T	−226.309 539	−134.2	2(A_g, A_u)	N/A(H_M→ Z_O)		
		aTZ	T	−226.324 776	−85.5	2(A_g, A_u)	N/A(H_M→ Z_O)		
		aCVTZ	T	−226.540 633	−81.1				
		aQZ	T	−226.381 074	−72.7	2(A_g, A_u)			
	CCSD(T)-F12b	aDZ	T	−226.357 885	−71.8	2	−226.357 784	−49.7	2
		aTZ	T	−226.386 119	−68.1	3	−226.386 072	−57.8	3
		aQZ	T	−226.403749	−65.3				
T-shaped, T_C(C_s)	MP2	aDZ	M	−226.110 969	−225.9	0	N/A(T_C→ Z_C)		
		aCVDZ	M	−226.265 866	−245.6	0	N/A(T_C→ Z_C)		
		aTZ	M	−226.285 682[b]	−188.7	0	N/A(T_C→ Z_C)		
		aQz	M	−226.346 638[b]	−174.0				
		a5Z	M	−226.368 638[b]	−160.9				
		aCVTZ	M	−226.494 698	−184.2	0	N/A(T_C→ Z_C)		
	MP2-F12	aDZ	M	N/A(T_C→ Z_C)			N/A(T_C→ Z_C)		
		aTZ	M	−226.374 529	−160.7	0	−226.374 434	−139.9	0
		aQZ	M	N/A(T_C→ Z_C)					
	CCSD(T)	aDZ	M	−226.149 079	−213.7	0	−226.148 593	−107.0	
		aCVDZ	M	−226.309 998	−235.1	0	−226.309 421	−108.3	
		aTZ	M	−226.325 178	−173.5	0	−226.324 931	−119.3	
		aCVTZ	M	−226.541 004	−162.7	0	−226.540 810	−120.1	
		aQZ	M	−226.381 423	−149.4		−226.381 319	−126.6	
	CCSD(T)-F12b	aDZ	M	−226.358 219	−145.1	0	−226.358 099	−118.8	0
		aTZ	M	–[b]			−226.386 388	−127.1	0
		aQZ	M	−226.404 081	−137.9	0	−226.404 048	−130.9	
T-shaped, T_O(C_s)	MP2	aDZ	M	N/A(T_O→ I_O)			−226.110 435	−108.6	0
		aTZ	M	N/A(T_O→ I_O)			−226.285 375	−121.4	0
		aQZ	M	N/A(T_O→ Z_O)			−226.346 411	−124.1	0
	MP2-F12	a5Z	M	N/A(T_O→ Z_O)					
	CCSD(T)	aDZ	M	−226.148 997	−195.7	0	−226.148 549	−97.3	0
		aCVDZ	M	−226.309 889	−211.0	0	−226.309 372	−97.1	0
		aTZ	M	−226.325 141	−165.4	0	−226.324 898	−112.1	0
		aCVTZ	M	−226.540 952	−151.0	0	−226.540 773	−112.0	0
		aQZ	M	−226.381 379	−139.8	0	−226.381 276	−117.1	
	CCSD(T)-F12b	aDZ	M	−226.358 204	−141.8	0	−226.358 060	−110.2	0
		aTZ	M	−226.386 434	−137.2	0	−226.386 376	−124.5	0
		aQZ	M	−226.404 039	−128.9	0	−226.404 000	−120.3	0

(*continued*).

Table 2. Continued.

Stationary point (symm.)	Level of theory	Basis	M/T	$E_{el}^{no\,CP}/E_h$	$\Delta E_{int}^{no\,CP}/cm^{-1}$	TS*n*(symm.)	E_{el}^{wCP}/E_h	$\Delta E_{int}^{w\,CP}/cm^{-1}$	TS*n*
V-shaped, $V_O(C_{2v})$	MP2	aDZ	M	N/A($V_O \rightarrow I_O$)			−226.110 425	−106.5	1
		aTZ	M	N/A($V_O \rightarrow I_O$)			−226.285 375	−121.3	0
		aQZ	M	−226.346 510	−145.8	1	−226.346 413	−124.4	0
		a5Z	M	−226.368 532	−137.7	0	−226.368 486	−127.5	
	MP2-F12	aDZ	M	−226.362 713	−145.0	0	−226.362 647	−130.7	0
		aTZ	M	−226.374 434	−139.9	0	−226.374 409	−134.4	0
		aQZ	M	−226.385 147	−131.5	0	−226.385 138	−129.5	0
		a5Z	M	−226.388 235	−131.7	2			
	CCSD(T)	aDZ	M	N/A($V_O \rightarrow I_O$)			−226.148 248	−31.1	2
		aTZ	M	N/A($V_O \rightarrow I_O$)			−226.324 621	−51.3	1
		aQZ	M	−226.381 065	−70.9	2	−226.380 999	−56.4	
	CCSD(T)-F12b	aDZ	M	−226.357 879	−70.5	1	−226.357 786	−50.1	1
		aTZ	M	−226.386 127	−69.8	1	−226.386 083	−60.3	1
		aQZ	M	−226.403 742	−63.7	1	−226.403 722	−59.3	1
		a5Z	M	−226.409 178	−62.3				
V-shaped, $V_C(C_{2v})$	MP2-F12	aDZ	M	N/A($V_C \rightarrow V_O$)					
		aTZ	M	N/A($V_C \rightarrow V_O$)					
		aQZ	M	N/A($V_C \rightarrow V_O$)					

Note: [a] See footnote *a* to Table 1. [b] Numerical stability issues.

related entries in Table 1). It is important to emphasise the very small energy difference between the $Z_O(C_{2h})$ and $Z_M(C_s)$ forms, pointing toward a late transition state. This, along with the problems mentioned for Z_C/T_C and Z_O/T_O, should present considerable difficulties for the generation of a spectroscopically accurate ground-state potential energy surface [101, 102] for the van der Waals dimer $(CO)_2$.

It emerged from geometry optimizations searching for minima that a rectangular H-shaped form with C_s point-group symmetry is not a minimum for the CO dimer. Optimizations toward a minimum, whether using a parallel or antiparallel initial H-shaped structure, have always resulted in stationary points with shapes different from H (e.g. linear (I) or Z). However, when a search was conducted for a TS, a stationary point with C_{2h} point-group symmetry could be found. These H-shaped stationary points turned out not to be first-order but rather second-order transition states. One of the imaginary modes connects the planar Z_C and Z_O forms, while the other mode corresponds to an out-of-plane displacement of the two monomer units, pointing toward shape X.

Based on the results obtained for the H-shaped second-order transition state (see Table 2), we were also searching for a first-order non-planar transition state of shape X. It has been found in the form of a stationary point having C_2 point-group symmetry. As expected, the electronic energy of the X-shaped form is always lower than that of H_M (see Table 2). However, the X-shaped form is not always a first-order transition state; sometimes, it is a second-order one. Optimising the dihedral angle, even with the C_2 symmetry constraint, turned out to be difficult at a number of levels due to the flatness of the potential. Sometimes two nearly isoenergetic stationary points were found (see Table 2). It is also remarkable, again due to the flatness of the PES, how different the optimised dihedral angle can be.

The T-shaped form T_O, with C_s point-group symmetry, is a minimum when the corresponding Z_O form, with C_{2h} point-group symmetry, is a first-order transition state. This occurs, for example, at the aug-cc-pVDZ CCSD(T) level. Similar comments can be made about the T_C-shaped SPs (*vide supra*); they are mostly included in Table 2 in cases when the 'corresponding' Z_C is not a minimum.

Curiously, at the standard frozen-core aug-cc-pVTZ MP2 level, the I_O form is determined to be a minimum, while the other two forms, I_C and I_M, are fourth-order transition states (see Table 3). Inclusion of the counterpoise correction in the energy calculation results in mostly fourth-order transition states. At the aug-cc-pV5Z MP2 level, there is no SP corresponding to I_C anymore, in accordance with the changes in $E_{el}^{no\,CP}$. Even more interesting is the fact that, with the CP correction, one cannot find an SP for the shape I_C. Thus, this provides another example of the dangers of using incomplete basis sets and lower levels of electronic structure theory for drawing conclusions during the determination of the SPs of the CO dimer. Clearly, at the highest levels of electronic structure theory, only two of the three possible linear forms, I_O and I_M, exist, and they appear to be higher-order transition states (we consistently obtain this picture when the CP correction is considered, though this picture is blurred somewhat by the F12 results). When the linear SPs have a Hessian index of four, they are characterised by two doubly degenerate, imaginary bending modes; only the stretching modes are real.

Table 3. Results of geometry optimizations yielding linear (shape I) stationary points[a].

Stationary point (symm.)	Level of theory	Basis	M/T	E_{el}^{noCP}/E_h	$\Delta E_{int}^{noCP}/cm^{-1}$	TS*n*	E_{el}^{wCP}/E_h	$\Delta E_{int}^{wCP}/cm^{-1}$	TS*n*
I-shaped, $I_O(D_{\infty h})$	MP2	aDZ	M	−226.110 934	−218.2	0	−226.110 381	−96.9	4
		aCVDZ	M	−226.265 814	−234.4	0	−226.265 188	−96.9	4
		aTZ	M	−226.285 626	−176.5	0	−226.285 297	−104.2	4
		aCVTZ	M	−226.494 534	−148.2	4	−226.494 327	−102.7	4
		aQZ	M	−226.346 480	−139.3	4	−226.346 322	−104.7	4
		aCVQZ	M	−226.570 418	−127.0	4	−226.570 313	−103.9	4
		a5Z	M	−226.368 439	−116.8	4	−226.368 387	−105.8	4
		aCV5Z	M	−226.596 263	−114.2	4	−226.596 222	−105.1	
		a6Z	M	−226.377 241	−115.8		−226.377 219	−111.0	
	MP2-F12	aDZ	M	−226.362 678	−137.3	0	−226.362 543	−107.7	0
		aTZ	M	−226.374 303	−111.1	4	−226.374 305	−111.5	—[b]
		aQZ	M	−226.385 054	−111.0	2	−226.385 033	−106.4	—[b]
		a5Z	M	−226.388 128	−108.3	—[b]	−226.388 123	−107.2	—[b]
	CCSD(T)	aDZ	M	−226.148 740	−139.2	0	−226.148 203	−21.4	1
		aCVDZ	M	−226.309 638	−155.9	0	−226.309 028	−22.0	1
		aTZ	M	−226.324 830	−97.2	2	−226.324 548	−35.3	1
		aCVTZ	M	−226.540 596	−73.1	2	−226.540 426	−35.8	0
		aQZ	M	−226.381 032	−63.7	2	−226.380 918	−38.6	0
		aCVQZ	M	−226.611 588	−55.7	2	−226.611 514	−39.4	0
		a5Z	M	−226.398 766	−46.7		−226.398 735	−39.9	2
		aCV5Z	M	−226.633 040	−45.8	—[b]	−226.633 016	−40.6	
	CCSD(T)-F12b	aDZ	M	−226.357 918	−78.0	0	−226.357 719	−35.4	0
		aTZ	M	−226.386 034	−49.4	2	−226.386 002	−42.4	—[b]
		aQZ	M	−226.403 677	−49.4	—[b]	−226.403 628	−38.7	
		a5Z	M	−226.409 090	−43.1		−226.409 080	−40.8	
I-shaped, $I_M(C_{\infty v})$	MP2	aDZ	M	−226.110 283	−75.4	2	−226.109 923	3.7	4
		aCVDZ	M	−226.265 153	−89.2	2	−226.264 732	3.2	4
		aTZ	M	−226.285 029	−45.4	4	−226.284 835	−2.8	4
		aCVTZ	M	−226.493 993	−29.4	4	−226.493 876	−3.8	4
		aQZ	M	−226.345 971	−27.7	2	−226.345 872	−5.7	4
		aCVQZ	M	−226.569 936	−21.1	4	−226.569 871	−6.8	
		a5Z	M	−226.367 965	−13.1	4	−226.367 936	−6.8	4
		aCV5Z	M	−226.595 801	−12.7	4	–		
		a6Z	M	−226.376 782	−15.0		–		
	MP2-F12	aDZ	M	−226.362 154	−22.3	2	−226.362 089	−8.1	3
		aTZ	M	−226.373 868	−15.6	—[b]	−226.373 835	−8.4	—[b]
		aQZ	M	−226.384 594	−10.2	—[b]	−226.384 577	−6.3	—[b]
		a5Z	M	−226.387 674	−8.6	—[b]	−226.387 670	−7.8	2
	CCSD(T)	aDZ	M	−226.148 580	−104.2	2	−226.148 181	−16.5	3
		aCVDZ	M	−226.309 468	−118.6	2	−226.309 001	−16.1	3
		aTZ	M	−226.324 694	−67.3	4	−226.324 483	−21.0	3
		aCVTZ	M	−226.540 482	−48.1	4	−226.540 356	−20.5	3
		aQZ	M	−226.380 935	−42.3	4	−226.380˙844	−22.4	
		aCVQZ	M	−226.611 495	−35.3	4	−226.611 434	−22.0	
		a5Z	M	−226.398 679	−27.6	4	−226.398 657	−22.8	
		aCV5Z	M	−226.632 950	−26.1		–		
	CCSD(T)-F12b	aDZ	M	−226.357 763	−45.0	2	−226.357 647	−19.6	3
		aTZ	M	−226.385 978	−37.2	3	−226.385 914	−23.1	—[b]
		baQZ	M	−226.403 586	−29.4	—[b]	−226.403 554	−22.4	—[b]
		a5Z	M	−226.409 006	−24.7	—[b]	−226.408 998	−22.9	
I-shaped, $I_C(D_{\infty h})$	MP2	aDZ	M	−226.110 037	−21.4	4	N/A(dissoc.)		
		aCVDZ	M	−226.264 880	−29.3	4	N/A(dissoc.)		
		aTZ	M	−226.284 900	−17.1	4	N/A(dissoc.)		
		aCVTZ	M	−226.493 871	−2.7	4	N/A(dissoc.)		
		aQZ	M	N/A(dissoc.)	–	–	N/A(dissoc.)		
		aCVQZ	M	N/A(dissoc.)	–	–			
		a5Z	M	N/A(dissoc.)	–	–			
		aCV5Z	M	N/A(dissoc.)	–	–			
	CCSD(T)	aDZ	M	−226.148 225	−26.2	4			
		aCVDZ	M	−226.309 096	−37.0	4			
		aTZ	M	−226.324 481	−20.5	4			
		aCVTZ	M	−226.540 278	−6.2	4			
		aQZ	M	N/A(dissoc.)	–	–			

Note: [a] See footnote *a* to Table 1. [b] Numerical stability issues.

Table 4. Structural parameters (distances r and R, angles $\angle$ and ϕ, total dipole moment μ_{tot}, and rotational constants A, B, and C) of the reference geometries used during the focal-point analysis of the electronic interaction energies characterising stationary points on the ground electronic state potential energy surface of $(^{12}C^{16}O)_2$ (the bond length of the free monomer, at the same level, is 1.1318 Å).

Structural parameter	$Z_C(C_{2h})$	$Z_O(C_{2h})$	$X(C_2)$	$I_O(D_{\infty h})$	$I_M(C_{\infty v})$
$r_{monomer}$/Å	1.1317	1.1320	1.132	1.1318	1.1320
$\angle_{COM-COM-C/O}$/deg	46.92	62.89	180.0	–	–
$R_{COM-COM}$/Å	4.246	3.723	3.887	4.372	5.036
ϕ/deg	180.0	180.0	25.8	–	–
μ_{tot}	0.0	0.0	0.14	0.0	0.23
A/cm^{-1}	1.959	1.186	0.970		
B/cm^{-1}	0.061	0.089	0.079	0.062	0.047
C/cm^{-1}	0.059	0.083	0.074		

Table 5. Focal-point analysis (FPA) table of the electronic interaction energies characterising the two Z-shaped forms, Z_C and Z_O, and the first-order transition state, Z_M, connecting the two stationary points on the ground electronic state potential energy surface of the CO dimer, both with and without the consideration of the counterpoise (CP) energy corrections.

Isomer	CP corr.	Basis	ΔE_e[HF]	δ[MP2]	δ[CCSD]	δ[CCSD(T)]	δ[CCSDT]	δ[CCSDT(Q)]	ΔE_e[FCI]
Z_C, global minimum (C_{2h})	no	aug-cc-pVDZ	+32.96	−248.68	+51.26	−36.22	−2.53	−1.49	−204.71
		aug-cc-pVTZ	+55.40	−241.63	+56.85	−34.47	[−2.53]	[−1.49]	[−167.88]
		aug-cc-pVQZ	+62.18	−234.43	+59.23	−34.81	[−2.53]	[−1.49]	[−151.85]
		aug-cc-pV5Z	+67.59	−227.48	+58.77	−34.69	[−2.53]	[−1.49]	[−139.84]
		aug-cc-pV6Z	+67.98	−225.38	+58.25	−34.76	[−2.53]	[−1.49]	[−137.93]
		CBS(3-4)	+63.04	−233.53	+59.53	−34.85			
		CBS(4-5)	+68.49	−226.32	+58.69	−34.68			
		CBS(5-6)	**+68.06**	**−224.94**	**+58.15**	**−34.78**	**−2.53**	**−1.49**	**−137.53**
		unc(3-4)	0.86	0.91	0.30	0.04			
		unc(4-5)	0.90	1.16	0.08	0.02			
		unc(5-6)	0.08	0.43	0.11	0.01			
	yes	aug-cc-pVDZ	+66.69	−193.87	+50.52	−26.89	−2.85	−1.73	−108.12
		aug-cc-pVTZ	+69.64	−210.50	+53.54	−31.94	[−2.85]	[−1.73]	[−123.85]
		aug-cc-pVQZ	+68.55	−217.04	+54.95	−33.65	[−2.85]	[−1.73]	[−131.77]
		aug-cc-pV5Z	+68.04	−219.81	+55.72	−34.29	[−2.85]	[−1.73]	[−134.91]
		aug-cc-pV6Z	+68.04	−221.24	+56.20	−34.58	[−2.85]	[−1.73]	[−136.17]
		CBS(3-4)	+68.41	−217.86	+55.13	−33.87			
		CBS(4-5)	+67.96	−220.27	+55.85	−34.40			
		CBS(5-6)	**+68.04**	**−221.54**	**+56.30**	**−34.64**	**−2.85**	**−1.73**	**−136.42**
		unc(3-4)	0.14	0.82	0.18	0.22			
		unc(4-5)	0.08	0.46	0.13	0.11			
		unc(5-6)	0.00	0.30	0.10	0.06			
Z_O, local minimum (C_{2h})	no	aug-cc-pVDZ	−3.42	−161.09	+14.76	−33.07	+5.38	−1.59	−179.03
		aug-cc-pVTZ	+23.81	−159.09	+18.25	−32.16	[+5.38]	[−1.59]	[−145.40]
		aug-cc-pVQZ	+31.99	−154.86	+20.08	−32.23	[+5.38]	[−1.59]	[−131.23]
		aug-cc-pV5Z	+36.27	−151.86	+20.45	−32.20	[+5.38]	[−1.59]	[−123.57]
		aug-cc-pV6Z	+36.56	−148.90	+19.49	−32.17	[+5.38]	[−1.59]	[−121.23]
		CBS(3-4)	+33.03	−154.33	+20.31	−32.24			
		CBS(4-5)	+36.98	−151.36	+20.51	−32.20			
		CBS(5-6)	**+36.62**	**−148.28**	**+19.30**	**−32.17**	**+5.38**	**−1.59**	**−120.74**
		unc(2-3)	2.25	0.17	0.29	0.08			
		unc(3-4)	1.03	0.53	0.23	0.01			
		unc(4-5)	0.72	0.50	0.06	0.00			
		unc(5-6)	0.06	0.61	0.20	0.01			
	yes	aug-cc-pVDZ	+30.29	−108.55	+11.24	−25.02	+5.43	−1.75	−88.35
		aug-cc-pVTZ	+34.34	−131.80	+14.40	−29.86	[+5.43]	[−1.75]	[−109.24]
		aug-cc-pVQZ	+36.68	−139.48	+16.01	−31.15	[+5.43]	[−1.75]	[−114.27]
		aug-cc-pV5Z	+36.70	−142.69	+16.89	−31.70	[+5.43]	[−1.75]	[−117.13]
		aug-cc-pV6Z	+36.63	−144.62	+17.46	−31.98	[+5.43]	[−1.75]	[−118.83]
		CBS(3-4)	+36.97	−140.45	+16.21	−31.32			
		CBS(4-5)	+36.70	−143.23	+17.04	−31.79			
		CBS(5-6)	**+36.62**	**−145.02**	**+17.57**	**−32.03**	**+5.43**	**−1.75**	**−119.18**
		unc(3-4)	0.29	0.97	0.20	0.16			
		unc(4-5)	0.00	0.54	0.15	0.09			
		unc(5-6)	0.01	0.40	0.12	0.06			

Note: [a] The symbol δ denotes the increment in the relative energy ΔE_e with respect to the preceding level of theory in the hierarchy HF → MP2 → CCSD → ⋯ → FCI. CBS = complete basis set, FCI = full configuration interaction. The basis set extrapolations are described in the text, they are based on the cardinal number X of the bases. unc(i, j) = uncertainty, based on extrapolation with energies obtained with basis sets of cardinal number i and j. The final energy values corresponding to the CBS limit are boldfaced. The final uncertainties are given in parentheses. All energy values are in (hc) cm^{-1}.

Table 6. Focal-point analysis table of the electronic interaction energies characterising further high-symmetry stationary points on the ground electronic state potential energy surface of the CO dimer (I_O and I_M are transition states of order 4).

Stationary point	CP corr.	Basis	ΔE_e[RHF]	δ[MP2]	δ[CCSD]	δ[CCSD(T)]	δ[CCSDT]	δ[CCSDT(Q)]	ΔE_e[FCI]
I-shaped, I_O ($D_{\infty h}$)	no	aug-cc-pVDZ	+29.99	−230.19	+76.49	−16.85	−10.35	+2.39	−148.52
		aug-cc-pVTZ	+71.94	−223.23	+77.49	−15.11	[−10.35]	[+2.39]	[−96.87]
		aug-cc-pVQZ	+93.54	−219.69	+80.43	−16.14	[−10.35]	[+2.39]	[−69.82]
		aug-cc-pV5Z	+97.26	−206.94	+78.70	−15.54	[−10.35]	[+2.39]	[−54.47]
		aug-cc-pV6Z	+97.81	−203.38	+77.63	−15.53	[−10.35]	[+2.39]	[−51.44]
		CBS(2-3)	+75.41	−222.65	+77.57	−14.97			
		CBS(3-4)	+96.27	−219.25	+80.80	−16.27			
		CBS(4-5)	+97.88	−204.80	+78.41	−15.44			
		CBS(5-6)	**+97.92**	**−202.65**	**+77.40**	**−15.53**	**−10.35**	**+2.39**	**−50.82**
		unc(2-3)	3.47	0.58	0.08	0.14			
		unc(3-4)	2.73	0.45	0.37	0.13			
		unc(4-5)	0.62	2.13	0.29	0.10			
		unc(5-6)	0.11	0.73	0.22	0.00			
	yes	aug-cc-pVDZ	+99.86	−186.50	+74.89	−9.11	−9.70	+2.21	−28.35
		aug-cc-pVTZ	+98.86	−196.36	+75.37	−13.40	[−9.70]	[+2.21]	[−43.02]
		aug-cc-pVQZ	+97.64	−196.89	+75.21	−14.66	[−9.70]	[+2.21]	[−46.19]
		aug-cc-pV5Z	+97.88	−198.12	+75.50	−15.14	[−9.70]	[+2.21]	[−47.36]
		aug-cc-pV6Z	+97.96	−198.74	+75.62	−15.35	[−9.70]	[+2.21]	[−48.01]
		CBS(2-3)	+98.78	−197.18	+75.41	−13.76			
		CBS(3-4)	+97.48	−196.95	+75.19	−14.82			
		CBS(4-5)	+97.92	−198.32	+75.55	−15.22			
		CBS(5-6)	**+97.97**	**−198.87**	**+75.65**	**−15.39**	**−9.70**	**+2.21**	**−48.13**
		unc(2-3)	0.08	0.81	0.04	0.35			
		unc(3-4)	0.15	0.07	0.02	0.16			
		unc(4-5)	0.04	0.21	0.05	0.08			
		unc(5-6)	0.02	0.13	0.03	0.04			
I-shaped, I_M ($C_{\infty v}$)	no	aug-cc-pVDZ	+31.03	−111.53	+2.38	−23.89	+8.03	−4.20	−98.18
		aug-cc-pVTZ	+54.71	−99.17	+3.10	−20.64	[+8.03]	[−4.20]	[−58.17]
		aug-cc-pVQZ	+68.34	−96.06	+7.26	−20.41	[+8.03]	[−4.20]	[−37.05]
		aug-cc-pV5Z	+72.31	−86.17	+6.22	−19.73	[+8.03]	[−4.20]	[−23.53]
		aug-cc-pV6Z	+72.86	−84.04	+5.78	−19.66	[+8.03]	[−4.20]	[−21.22]
		CBS(2-3)	+56.67	−98.15	+3.16	−20.37			
		CBS(3-4)	+70.06	−95.67	+7.79	−20.38			
		CBS(4-5)	+72.98	−84.51	+6.05	−19.62			
		CBS(5-6)	**+72.97**	**−83.60**	**+5.70**	**−19.64**	**+8.03**	**−4.20**	**−20.74**
		unc(2-3)	1.96	1.02	0.06	0.27			
		unc(3-4)	1.72	0.39	0.53	0.03			
		unc(4-5)	0.67	1.66	0.17	0.11			
		unc(5-6)	0.011	0.44	0.09	0.02			
	yes	aug-cc-pVDZ	+73.67	−72.92	+0.37	−17.46	+8.11	−4.58	−12.80
		aug-cc-pVTZ	+72.97	−77.24	+2.13	−19.02	[+8.11]	[−4.58]	[−25.73]
		aug-cc-pVQZ	+72.70	−79.22	+3.54	−19.31	[+8.11]	[−4.58]	[−26.87]
		aug-cc-pV5Z	+72.93	−80.26	+4.08	−19.46	[+8.11]	[−4.58]	[−27.29]
		aug-cc-pV6Z	+72.97	−80.71	+4.31	−19.52	[+8.11]	[−4.58]	[−27.54]
		CBS(2-3)	+72.91	−77.60	+2.28	−19.15			
		CBS(3-4)	+72.67	−79.47	+3.72	−19.34			
		CBS(4-5)	+72.97	−80.43	+4.17	−19.49			
		CBS(5-6)	**+72.98**	**−80.80**	**+4.35**	**−19.53**	**+8.11**	**−4.58**	**−19.45**
		unc(2-3)	0.06	0.36	0.15	0.13			
		unc(3-4)	0.03	0.25	0.18	0.07			
		unc(4-5)	0.04	0.17	0.09	0.03			
		unc(5-6)	0.01	0.09	0.05	0.01			

As for shape V, with an equilibrium structure of C_{2v} point-group symmetry, the initial V_C arrangement of the atoms has never resulted in a SP of this shape, the optimizations always ended up with shape V_O. Shape V_O has turned out to be a minimum at certain levels of theory and a relatively low-energy one (see Table 2). When linear I_O is a minimum at the MP2 level, the SP corresponding to V_O could not be located (this $V_O \rightarrow I_O$ rearrangement is allowed within the C_{2v} point group). Curiously, this is not the case at the MP2-F12 level.

As expected, the convergence of the interaction energies obtained with the explicitly correlated (F12) calculations toward the CBS limits is significantly faster than that of the traditional results; however, in many cases, the convergence is not smooth. The differences between the traditional and the F12 results are especially notable for

Table 7. Interaction energy components at various levels of SAPT approximations (aug-cc-pV5Z basis set) for selected stationary points of the CO dimer (Z_C, Z_O, Z_M, and T_O) in its ground electronic state, all results are in (hc) cm^{-1}.

	$Z_C(C_{2h})$	$Z_O(C_{2h})$	$Z_M(C_s)$	$T_O(C_s)$
Electrostatics				
SAPT0	−81.5	−107.5	−66.7	−94.2
SAPT(DFT)	−111.5	−62.2	−62.1	−73.6
SAPT2+3(CCD)	−108.4	−60.5	−63.9	−68.5
Exchange				
SAPT0	178.9	138.5	156.0	123.4
SAPT(DFT)	200.0	149.4	174.0	152.0
SAPT2+3(CCD)	185.0	148.9	167.9	144.2
Induction				
SAPT0	−23.7	−8.6	−14.1	−13.3
SAPT(DFT)	−23.1	−6.4	−12.0	−10.3
SAPT2+3(CCD)	−23.3	−8.5	−14.0	−13.3
Dispersion				
SAPT0	−203.7	−218.5	−221.1	−198.4
SAPT(DFT)	−208.9	−201.0	−213.5	−187.6
SAPT2+3(CCD)	−213.6	−209.1	−221.8	−193.3
Total				
SAPT0	−130.0	−196.2	−146.0	−182.5
SAPT(DFT)	−143.6	−120.1	−113.6	−119.5
SAPT2+3(CCD)	−160.3	−129.2	−131.8	−130.7

the smallest (DZ and TZ) basis sets. It is also worth noting that by the time the QZ basis sets are used, the difference between the CP-uncorrected and the CP-corrected F12 results diminishes: for example, with the aug-cc-pV5Z basis set, at the MP2-F12 level, the absolute differences for the Z_C, Z_O, I_O, and I_M shapes are 5.6, 1.9, 1.1, and 0.8 cm^{-1}, respectively. The CCSD(T)-F12b differences are often larger than those characterising the MP2-F12 results.

As expected [60, 61], and as a rule, core-core and core-valence electron correlations do not play a qualitative role in the character of the stationary points (see Tables 1–3). All-electron treatments somewhat change the relative energies of the SPs, but as the basis set gets larger, the relative energy differences between the frozen-core and all-electron treatments become rather small (though they remain slightly larger than 1 cm^{-1}). The most important exceptions are the cases of Z_C with DZ-type basis sets and I_O with TZ-type basis sets, whereby the frozen-core treatment finds a spurious transition state and a minimum at the MP2 level, respectively. These unphysical results are 'corrected' at the all-electron level.

In summary, the following conclusions can be drawn about the stationary points, which are relevant for a future accurate calculation of a ground electronic state PES for the CO dimer: (a) there are two nearly isoenergetic minima on the PES, Z_C/T_C and Z_O/T_O; (b) at levels of theory where the Z_C and Z_O forms with an equilibrium structure of C_{2h} symmetry are not minima, there is a nearly isoenergetic nearby minimum with C_s point-group symmetry; (c) the equilibrium structure of the first-order transition state connecting the two minima, Z_M, has C_s point-group symmetry; (d) correction for BSSE through the CP (Boys–Bernardi) scheme is important and yields significantly better relative energies and qualitatively correct stationary points; (e) consideration of explicit (F12) electron correlation provides results that converge rapidly to the complete basis set limit; and (f) core-valence and core-core correlations are not important from a qualitative point of view and are barely important quantitatively.

3.2. Structural results

Reference [103] lists a large number of accurate *ab initio* results for the lengths of CO bonds in a variety of molecules. This reference provides a discussion of the effects that the augmentation of the basis set with diffuse functions, as well as the core-core and core-valence contributions, has on the CO bond lengths. The conclusions of Ref. [103] are clearly in line with the geometry optimisation results of this study. Careful studies of the equilibrium structure of van der Waals dimers also exist; see, for example, Ref. [104].

Selected structural parameters of the reference geometries, obtained at the frozen-core, CP-corrected aug-cc-pVQZ CCSD(T) level following complete geometry optimizations and used during the FPA analysis, are provided in Table 4. Table 4 also contains structural parameters used during the SAPT analysis of the bonding in the CO dimer (see also the supplementary tables to this paper).

The well-accepted value of the equilibrium bond length [105], r_e, for the monomer CO is 1.1287 Å [103, 106]. As usual, the larger the Gaussian basis set used, the shorter the optimised bond distance. At the MP2 level, the bond distance of the CO monomer in the Z-shaped dimers, in Å, changes between 1.1502 (frozen-core, aug-cc-pVDZ) and 1.1316 (all-electron, aug-cc-pCV5Z). At the CCSD(T) level, the comparable values are 1.1473 (frozen-core, aug-cc-pVDZ) and 1.1284 Å (all-electron, aug-cc-pCV5Z). Core-core and core-valence correlation decrease the bond length by 0.0027 and 0.0025 Å at the MP2 and CCSD(T) levels, respectively, more or less irrespective of the cardinal number of the basis. Close agreement with $r_e(CO) = 1.1287$ Å is obtained at the all-electron aug-cc-pCVQZ CCSD(T) level, where the optimised bond length is 1.1293 Å.

It is of interest to discuss the extent of the change in the monomer CO bond distance upon dimer formation. Irrespective of the actual shape of the stationary point, the change in the CO bond length is minuscule. For example, at the all-electron aug-cc-pCVQZ CCSD(T) level, the monomer's r_e bond length is 1.1293 Å, while it is 1.1291 Å

and 1.1295 Å in the $Z_C(C_{2h})$ and $Z_O(C_{2h})$ forms, respectively. Thus, there is a small but definitive contraction and elongation of the CO bond in the possible global and local minima, respectively. This observation holds for the reference geometries used for the FPA study, as well (see Table 4). It is also important to point out that even in the case of transition states, the monomer bond lengths change by a relatively small amount, significantly less than 0.001 Å (see Table 4).

While the relative energies and characteristics of the minima and the different-order transition states change at different levels, the bond lengths change rather little (see Table 4). Furthermore, the COM–COM distances, $R_{COM-COM}$, of the $Z_C(C_{2h})$ and $Z_O(C_{2h})$ forms are significantly different, see Table 4, and the values are rather similar at other levels of electronic structure theory. As observed earlier [33], the COM–COM distance is significantly larger at the global minimum than at the local minimum (see the further discussion in Section 3.4).

The two Z-shaped forms on the PES of the CO dimer, $Z_C(C_{2h})$ and $Z_O(C_{2h})$, are asymmetric tops (see Table 4), and the forms $T_C(C_s)$ and $T_O(C_s)$ are also asymmetric tops. The A rotational constants are relatively large: 1.98 and 1.19 cm^{-1} for $Z_C(C_{2h})$ and $Z_O(C_{2h})$, respectively. However, the B/C rotational constants are small, only 0.061/0.059 and 0.089/0.083 cm^{-1} for Z_C and Z_O, respectively. The B and C rotational constants are almost equal, indicating that the isomers are nearly symmetric tops.

Using a simplified model, rotational constants B have been deduced experimentally for several so-called 'stacks' of rotational transitions; [1, 21] these constants have been found to be about 0.060–0.064 and 0.072–0.078 cm^{-1} for the two isomers. The model values are in reasonable agreement with the calculated ones. Note that at the harmonic-oscillator approximation level, both the $Z_C(C_{2h})$ and $Z_O(C_{2h})$ forms have one very low vibrational wavenumber of B_u symmetry, about 4 and 8 cm^{-1}, respectively. It is worth noting that while the shape $T_O(C_s)$ is drastically different from the shape $Z_O(C_{2h})$, $T_O(C_s)$ is also a nearly symmetric-top form with B and C rotational constants of about 0.075 cm^{-1}, which is very close to the experimentally-deduced B value of the secondary minimum. The A rotational constant of $T_O(C_s)$, at about 1.98 cm^{-1}, is very different from that of $Z_O(C_{2h})$.

3.3. FPA analyses of the interaction energies

Two types of FPA analyses have been performed in this study to determine the relative energies of the selected stationary points on the ground electronic state PES of the CO dimer. Following the traditional FPA method (see, for example, Refs. [102, 107–110]), no CP correction was considered in the first set of calculations. Then, following Ref. [73], CP-corrected energies have also been obtained at all levels of theory considered, namely HF, MP2, and various versions of the coupled-cluster technique. The FPA results obtained are given in Tables 5 and 6 for the high-symmetry Z- and I-shaped forms, respectively.

As indicated by previous studies, at the traditional Hartree–Fock level, the energies of the stationary points on the PES of the ground electronic state of the CO dimer do not necessarily indicate binding. Nevertheless, the convergence of the relative energies to the physically incorrect CBS HF limit is usually as rapid as that for molecules with simpler electronic structures. It is only at correlated levels of electronic structure theory that the stationary points, with or without consideration of the counterpoise correction, become bound (i.e. have negative electronic interaction energies, see Tables 5 and 6).

It is important to point out that the traditional and the CP-corrected relative interaction energies, obtained using different basis sets at the MP2 level, converge to the CBS limit from different directions. The convergence of the CP-corrected relative energies is also significantly faster than that without the CP correction. All this is in accordance with the results of Ref. [50]. An important result of the geometry optimisation on the CO dimer is that it is preferable to use counterpoise correction during the geometry and quadratic force field computations, as this is seemingly a good way to ensure the qualitative correctness of the computed results, both at the MP2 and CCSD(T) levels, when basis sets of limited quality are used.

It is particularly interesting to study the effect of the counterpoise correction on the interaction energies and their convergence toward the complete basis set full configuration interaction (CBS FCI) limit [102]. The expectation is that as the basis sets get larger, the CP correction becomes less and less important. This holds in the present case as well. By assigning a two times larger weight to the CP-corrected CBS FCI value due to its faster convergence, the frozen-core electronic interaction energy of Z_C is $-(hc)136.8(15)$ cm^{-1}. This value is significantly different from that of some earlier computational studies; for example, Rode et al. [12] reported $-(hc)157$ cm^{-1}, which has a difference of 15% from the present value. The frozen-core electronic interaction energy of the Z_O isomer is $-(hc)119.7(20)$ cm^{-1}; thus, the electronic energy difference between the two isomers of the CO dimer is $-(hc)17.1(25)$ cm^{-1}. As expected, both interaction energy values are somewhat larger than the electronic interaction energy of the isoelectronic nitrogen dimer,

$-(hc)109.3(26)\ cm^{-1}$ [73]. The relation of these values and that of the heterodimer CO–N_2 has been discussed in Ref. [23].

Most of the time, core-core and core-valence corrections provide a very minor, almost negligible contribution to the relative energies. Thus, this small correction term could be excluded during the generation of an accurate PES for the CO dimer.

The scalar relativistic corrections (MVD1) [75] turned out to be negligible for the relative energies of the stationary points. For example, the MVD1 energy correction to the energy difference between the global (Z_C) and local (Z_O) minima, computed at the all-electron aug-cc-pCVTZ CCSD(T) level, is $(hc)0.14\ cm^{-1}$. For all the interaction energies, the relativistic contribution can be estimated as $(hc)0.0(0.2)\ cm^{-1}$, where the expanded (two-sigma) uncertainty is given in parentheses. Thus, it is clear that the relative relativistic energy corrections can be practically neglected when the ground-state PES of the CO dimer is generated.

Since the CO dimer is a relatively heavy system, it is expected that the diagonal Born–Oppenheimer correction (DBOC) will not change significantly along the PES. This has been checked at the RHF, MP2, and CCSD levels of electronic structure theory using several basis sets. It has always been found that while the DBOC energy correction is large, approximately $(hc)1800\ cm^{-1}$, the correction differences for the stationary points are small, sometimes much smaller than $(hc)0.1\ cm^{-1}$. Thus, the relativistic and DBOC corrections can safely be ignored during the survey of the relative energies of the stationary points on the ground electronic state PES of the CO dimer, their combined effect is only $(hc)0.0(2)\ cm^{-1}$.

The largest remaining uncertainty in the relative energies comes from the zero-point vibrational energies, which cannot be determined accurately from the harmonic force fields computed in this study [73]. Nevertheless, it is of interest to observe how much the relative ZPVE corrections change as the level of theory changes. Harmonic ZPVE values are compared at the MP2 level. One can clearly establish that the Z_C isomer always has a larger ZPVE value by about $(hc)30\ cm^{-1}$ than the Z_O isomer. Due to the four large-amplitude motions of the dimer, which cannot be adequately described by the harmonic oscillator approximation, this value has a large uncertainty but suggests that the well around the global minimum is tighter than that around the local one. This also means that the ZPVE correction on the relative energies has the opposite sign of the pure electronic difference, suggesting that the energy difference between the two isomers could indeed be minuscule, as observed experimentally.

3.4. SAPT analysis

It is of general interest to develop a physical interpretation of the intermolecular interactions and forces present in the CO dimer in terms of electrostatics, as well as exchange, induction, dispersion, and intramonomer correlation effects. For this energy decomposition, elements of symmetry-adapted perturbation theory [62, 80, 111] can be used.

The CO dimer has already been the subject of SAPT investigations and has become a standard model for testing increasingly sophisticated many-electron SAPT formulations. Rode and co-workers [12] performed the first detailed SAPT analysis of the interaction energy, highlighting the strong geometry dependence of the electrostatic term and its important role in determining the preferred orientations of the dimer, as well as its high sensitivity to intramonomer correlation effects. Vissers et al. [28] employed SAPT(DFT) to construct a four-dimensional potential energy surface to supplement microwave spectroscopy studies of the CO dimer. In their work, the SAPT(DFT) potential was found to be somewhat deeper around the global minimum than the corresponding CCSD(T) surface obtained using the same basis set. No decomposition of the SAPT interaction energy into individual components was reported. In several studies, individual SAPT components have been examined at selected geometries. For example, Korona et al. [20] demonstrated that effects usually regarded as small, such as orbital relaxation in the density matrices entering the SAPT expressions, can contribute as much as 30% of the exchange energy, corresponding to about 20% of the total interaction energy. Here, we are revisiting the SAPT analysis, including newly calculated stationary points of the CO dimer. The results are compared with those of the FPA analysis based on the best *ab initio* methods. The discussion below refers to Table 7, which collects the results of SAPT calculations using SAPT0, SAPT2+3(CCD), and SAPT(DFT), all obtained with the aug-cc-pV5Z basis set.

A qualitative understanding of the relative energy order of at least some of the stationary points on the PES of the CO dimer, as well as the energy order of the two minima, must be based on the alignment of the small dipole moments of the two monomer CO units. Based simply on the electronegativities of C and O, one expects that, in the CO monomer, the partial positive charge is on the carbon atom and the partial negative charge is on the oxygen atom. In contrast to this simplified picture, which mixes scalar quantities (charges) with vectorial ones (dipole moments), the direction of the small dipole moment of CO, 0.122 D [112], arises from the carbon atom carrying the negative end. This can only

be explained by the careful use of molecular orbital theory; a highly educational account of this can be found in Ref. [113]. Actually, for our discussion, it is only important to note the charge separation in the CO monomer, which affects how two (or more) CO units can interact. It is therefore convenient to start the discussion of the interaction mechanism from the electrostatic contribution, which is usually a key factor responsible for the differences in the energies between the stationary points of vdW dimers.

The value and direction of the electric dipole moment of the CO molecule are notoriously sensitive to the level of *ab initio* description [113, 114]. Consequently, the electrostatic term in SAPT is strongly affected by the choice of monomer densities, and the differences between SAPT0 and the correlated variants, in this case SAPT(DFT) and SAPT2+3(CCD), are substantial. For the Z_C configuration, SAPT0, which represents electrostatics computed from Hartree–Fock densities, recovers only about 73% of the SAPT(DFT) and SAPT2+3(CCD) electrostatic energy. For the Z_O configuration, the effect is opposite and even larger: the HF-based electrostatic energy overestimates the correlated value by roughly 70%. Since the dipole moment of CO is rather small, the long-range interaction, viewed purely as a multipole-multipole interaction in the region of the minima, is also modest. The dominant electrostatic contribution arises instead from short-range charge-penetration effects due to the close proximity of the monomers. The electrostatic interaction also varies substantially among the stationary points: when evaluated using DFT or correlated wave-function densities, it is nearly twice as attractive in Z_C as in Z_O. This behaviour is consistent with a more diffuse and overlapping electron density on the carbon end of CO, which enhances charge-penetration effects in the Z_C minimum.

The exchange (Pauli) repulsion tracks the extent of intermonomer density overlap, and its large magnitude in the minimum confirms the strong charge-penetration character of the interaction. Its magnitude is larger in the Z_C configuration ($\approx (hc)200\,\mathrm{cm}^{-1}$) than in the Z_O ($\approx (hc)150\,\mathrm{cm}^{-1}$) configuration, which confirms our conclusion regarding the electrostatic interaction: the electron's overlap is stronger when the carbon ends are in contact. The exchange interaction is less sensitive to the description of intramonomer correlation, and the deviations of both SAPT(DFT) and SAPT2 from SAPT0 are within 10%.

In the CO dimer, the induction effects, calculated here as the sum of induction and exchange-induction, are modest. This can be attributed to the small polarisability of this molecule: benchmark calculations [115] at the aug-cc-pVTZ CCSDT level yield 11.843 for $\alpha_{xx} = \alpha_{yy}$ and 15.497 for α_{zz}. Nonetheless, given the significant cancellation of many effects in the CO dimer, the induction energy, despite being small, contributes significantly to the difference in the depths of the Z-shaped minima.

As far as the main binding mechanism is concerned, the CO dimer is stabilised predominantly by dispersion interactions, which provide the main attractive contribution, whereas electrostatic interactions play a secondary role in determining the overall depth of the potential. As illustrated in Table 7 and Figure 1, the attractive dispersion term is fairly insensitive to the geometry and to the SAPT variant: for all stationary points and all three levels of theory, it lies between about $-(hc)190$ and $-(hc)220\,\mathrm{cm}^{-1}$, with SAPT2+3(CCD) yielding the most attractive values. The SAPT(DFT) dispersion energies are systematically intermediate between SAPT0 and SAPT2+3(CCD) and track the correlated CCD-based results closely, typically within a few tens of $(hc)\,\mathrm{cm}^{-1}$. This confirms that dispersion sets the overall scale of the CO dimer binding, while the differences between stationary points must arise primarily from other components, most notably from the interplay between electrostatics and exchange.

Note also that the polarisability of CO is not nearly as sensitive to the level of *ab initio* theory as its dipole moment: at the Hartree–Fock level, the polarisability underestimates the CCSDT reference by only about 6%, whereas MP2 and CCSD reproduce it to within about 1% (cf. Table III of Ref. [115]). This explains the relatively weak dependence of the second-order induction and dispersion corrections on the detailed treatment of intra-monomer correlation.

The wave-function-based SAPT interaction energies do not agree well with the supermolecular benchmarks. In particular, the overestimation of the interaction energy at the SAPT2+3(CCD) level, compared to CCSD(T), is unexpectedly large and suggests that further improvements in the SAPT treatment of intramonomer correlation and/or higher-order contributions are required for truly high accuracy.

The exchange (Pauli) component is especially sensitive to the treatment of intra-monomer correlation: the SAPT(DFT) exchange term is more repulsive than the SAPT2+3(CCD) value by about $(hc)15\,\mathrm{cm}^{-1}$. This trend is consistent with coupled-cluster benchmarks for exchange reported by Korona [116], who showed that SAPT(DFT) can be comparable in accuracy to wavefunction approaches based on CCSD density matrices (which are not available in the present `PSI4` implementation).

Furthermore, SAPT2+3(CCD) relies on estimated third-order contributions that remain sizable. For example, the Hartree–Fock correction $\delta^{(2)}_{\mathrm{HF}}$ is on the order of

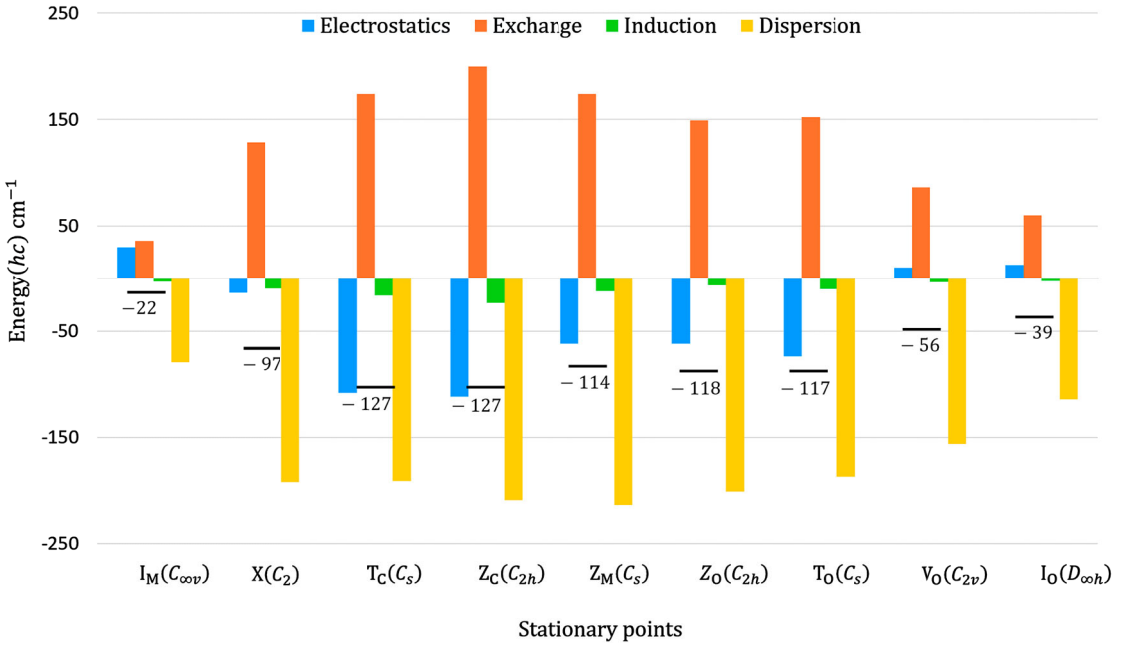

Figure 1. Interaction energy components for nine stationary points on the ground electronic state potential energy surface of the CO dimer. The plot shows the electrostatic, exchange, induction, and dispersion terms obtained using the SAPT(DFT) with the PBE0 functional and the aug-cc-pV5Z basis set. For reference purposes, total interaction energies calculated at the frozen-core aug-cc-pVQZ CCSD(T) level with counterpoise correction are presented for each stationary point.

$(hc)14\,\mathrm{cm}^{-1}$ (not shown in the tables). Because $\delta^{(2)}_{\mathrm{HF}}$ is defined at the HF level, it does not incorporate intra-monomer correlation, which may therefore remain a non-negligible source of error in both wave-function SAPT and SAPT(DFT). In contrast, SAPT(DFT)/PBE0 yields significantly better agreement with CCSD(T), overbinding by 4.3% for Z_C and by less than 1% for Z_O.

Finally, let us try to rationalise why the Z_M structure, despite the preferential interaction between the negative and positive ends of the monomers, is the least stable among the Z-shaped configurations. At the SAPT(DFT) level, the electrostatic stabilisation of Z_M, $-(hc)62.1\,\mathrm{cm}^{-1}$, is essentially identical to that of Z_O, $-(hc)62.2\,\mathrm{cm}^{-1}$, even though the monomer dipoles are oppositely aligned in the two structures. Z_M benefits from additional attractive contributions arising from induction, $-(hc)12.0\,\mathrm{cm}^{-1}$, and dispersion, $-(hc)213.5\,\mathrm{cm}^{-1}$, both of which are stronger than in Z_O, $-(hc)6.4$ and $-(hc)201.0\,\mathrm{cm}^{-1}$, respectively. However, these favourable effects are more than offset by a substantially larger exchange repulsion term in Z_M, $+(hc)174.0\,\mathrm{cm}^{-1}$, compared to $+(hc)149.4\,\mathrm{cm}^{-1}$ for Z_O. This increase is consistent with a greater overlap of the intermolecular electron densities and, consequently, stronger Pauli repulsion. The exchange energy of Z_M falls between those of Z_C and Z_O, as expected for an intermediate degree of electronic-cloud overlap. As a result of this delicate balance among interaction components, the total SAPT(DFT) interaction energy of Z_M is the least negative in the series, $-(hc)113.6\,\mathrm{cm}^{-1}$, rendering it the least stable Z-shaped configuration. It is worth emphasising that the cancellation among the individual interaction energy components is subtle: while SAPT(DFT) correctly predicts Z_M to be the least stable *Z* configuration, in agreement with high-level CCSD(T) benchmark results, SAPT0 and SAPT2+3(CCD) fail to reproduce this ordering.

4. Conclusions

The principal aim of this computational study was to conduct a comprehensive survey of the stationary points on the 'mysterious' CO dimer's ground electronic state potential energy surface. In total, a dozen stationary-point shapes were investigated. Numerical results are presented for 11 feasible geometrical motifs, where 'feasible' denotes structures that were identified as stationary points (minima or transition states with nonzero Hessian indices) by the electronic-structure methods employed.

For this tetratomic dimer, the geometrical motifs are denoted in this study by the letters H, I (linear), T, V, X (the only non-planar stationary point), and Z, listed in alphabetical order. Because the monomers contain two non-equivalent atoms, each motif admits two or three

distinct variants, which are distinguished by subscripts indicating the atoms in closest contact (C for carbon-carbon, O for oxygen-oxygen, and M for mixed carbon-oxygen). Occasionally, the point-group symmetry of the equilibrium structure is indicated in parentheses.

The electronic structure of carbon monoxide (CO), featuring a triple bond that is unusual for both constituent atoms, has long served as a testing ground for modern chemical-bonding theories [113]. Likewise, the complex electronic structure of the CO dimer poses significant challenges for (a) the determination and characterisation of the stationary points on the ground electronic state, as it suffers from a polytopic [68] landscape: at some levels of theory, the shapes $Z_C(C_{2h})$, $Z_O(C_{2h})$, $T_C(C_s)$, $T_O(C_s)$, $V_O(C_{2v})$, and $I_O(D_{\infty h})$ are all found to be minima, and (b) a qualitative understanding of its bonding. Notably, not only the MP2 but even the gold-standard CCSD(T) calculations can yield ambiguous conclusions regarding whether a given stationary point should be considered a minimum or a transition state. The application of counterpoise corrections and the use of explicitly correlated (F12) methods help to resolve most of the stability issues, but not all of them.

Consistent with recent high-level *ab initio* studies, our results confirm the existence of two isomers of the CO dimer, the global minimum adopting a Z-shaped, planar, slipped, antiparallel arrangement, Z_C. The $Z_C(C_{2h})$ structure is often predicted to be a first-order transition state, leading to an almost isoenergetic minimum, which can be described as $Z_C(C_s)$. As for the additional, secondary minimum, for $Z_O(C_{2h})$ the situation is somewhat similar to that of $Z_C(C_{2h})$; however, in this case, the equilibrium structure with C_s point-group symmetry is better described as having a shape $T_O(C_s)$. Comparison of the calculated and experimentally derived rotational constants suggests that the secondary minimum has the shape $T_O(C_s)$. A third Z-type configuration, Z_M, features a mixed CO contact. This structure is always a first-order transition state with C_s point-group symmetry, and it is at the top of the pathway connecting the two minima.

Almost without exception, the further stationary points identified on the ground electronic state surface of $(CO)_2$ have a Hessian index of at least 2. The only non-planar form, $X(C_2)$, has a relatively large interaction energy and it appears to be a second-order transition state. The stationary point with the shape $V_O(C_{2v})$ also appears to be a relatively stable one.

To achieve high accuracy for the relative energies of the stationary points – and to obtain conservative uncertainty estimates – the composite focal-point analysis (FPA) methodology was employed. Several stationary points on the ground electronic state of the CO dimer were examined within this framework. The most significant findings can be summarised as follows: (a) the inclusion of the counterpoise correction in the energy evaluations is essential for obtaining even qualitatively correct stationary points at multiple levels of theory, including the gold-standard CCSD(T) approach; (b) the counterpoise-corrected energies exhibit markedly improved convergence behaviour, approaching the complete-basis-set limit from the opposite direction relative to the uncorrected values; (c) explicitly correlated (F12) calculations display substantially better basis-set convergence than their conventional counterparts; (d) because the monomers' core electrons undergo only negligible changes upon dimer formation, core-core, core-valence, and relativistic contributions to the ground-state PES can be safely neglected for all practical purposes; and (e) although the diagonal Born–Oppenheimer correction is sizable, it varies only minimally across the PES for this relatively heavy four-atom system.

The electronic interaction energy of the global minimum is $-(hc)136.8(15)\,\mathrm{cm}^{-1}$, while the electronic energy difference between the global and local minima is only $(hc)17.1(25)\,\mathrm{cm}^{-1}$ (the underlying calculations were carried out at higher-symmetry reference structures). The harmonic zero-point vibrational energy corrections computed in this study to characterise the stationary points are highly approximate; the accurate FPA energy values can only be corrected for vibrational effects by the results of variational nuclear motion computations.

The nature of the CO· · ·CO intermolecular interactions was elucidated with the help of three different levels of symmetry-adapted perturbation theory: SAPT0, SAPT2+3(CCD), and SAPT(DFT). The best SAPT computations utilised the aug-cc-pV5Z basis set and were performed for the following nine stationary points (in alphabetical order): $I_M(C_{\infty v})$, $I_O(D_{\infty h})$, $T_C(C_s)$, $T_O(C_s)$, $V_O(C_{2v})$, $Z_C(C_{2h})$, $Z_M(C_s)$, $Z_O(C_{2h})$, and $X(C_2)$. A detailed interaction-energy analysis, involving electrostatics, exchange, induction, and dispersion terms, explains the bonding in the CO dimer as primarily arising from dispersion rather than electrostatics. The same calculations indicate that the CO dimer provides a non-trivial case for SAPT analyses; thus, further improvements in the SAPT treatment of intra-monomer correlation and/or higher-order contributions are required to achieve truly high accuracy.

Acknowledgments

This paper is dedicated to Professor Frédéric Merkt, a friend and colleague of the corresponding author, with whom they share many scientific interests and have enjoyed numerous

stimulating discussions over the years, particularly on high-resolution and precision spectroscopy. AGC thanks Prof. G. Rauhut for his help with some of the MOLPRO runs.

Data availability statement

The authors confirm that the data supporting the findings of this study are available within the article and its supplementary materials. Further raw data supporting this study are available from the corresponding author (AGC) on request.

Disclosure statement

No potential conflict of interest was reported by the author(s).

Funding

The major support for the research described came from the MSCA Doctoral Network PHYMOL, 'Physics, Accuracy and Machine Learning: Towards the Next Generation of Molecular Potentials'. The project also received funding from the National Research, Development, and Innovation Office of Hungary (NKFIH, grants no. K138233 and 152791 to AGC). The results support the research of the COST Action CA21101 'Confined molecular systems: from a new generation of materials to the stars' [COSY, funded by the European Cooperation in Science and Technology (COST)].

References

[1] L. Surin, D.N. Fourzikov, F. Lewen, B.S. Dumesh, G. Winnewisser and A. McKellar, J. Mol. Spectrosc.**222**, 93–101 (2003). doi:10.1016/S0022-2852(03)00023-7
[2] P.A. Vanden Bout, J.M. Steed, L.S. Bernstein and W. Klemperer, Astrophys. J. **234**, 503–505 (1979). doi:10.1086/157522
[3] A. van der Pol, A. van der Avoird and P.E.S. Wormer, J. Chem. Phys. **92**, 7498–7504 (1990). doi:10.1063/1.458185
[4] P.R. Bunker, P. Jensen, S.C. Althorpe and D.C. Clary, J. Mol. Spectrosc. **157**, 208–219 (1993). doi:10.1006/jmsp.1993.1017
[5] R.W. Randall, A.J. Cliffe, B.J. Howard and A.R.W. McKellar, Mol. Phys. **79**, 1113–1126 (1993). doi:10.1080/00268979300101871
[6] M. Havenith, M. Petri, C. Lubina, G. Hilpert and W. Urban, J. Mol. Spectrosc. **167**, 248–261 (1994). doi:10.1006/jmsp.1994.1232
[7] C. Hattig, G. Jansen, B.A. Hess and J.G. Ángyán, Mol. Phys. **91**, 145–160 (1997). doi:10.1080/002689797171841
[8] M.D. Brookes and A.R.W. McKellar, Chem. Phys. Lett. **287**, 365–370 (1998). doi:10.1016/S0009-2614(98)00171-7
[9] A.W. Meredith and A.J. Stone, J. Phys. Chem. A **102**, 434–445 (1998). doi:10.1021/jp972114b
[10] D.A. Roth, M. Hepp, I. Pak and G. Winnewisser, Chem. Phys. Lett. **298**, 381–384 (1998). doi:10.1016/S0009-2614(98)01230-5
[11] M.D. Brookes and A.R.W. McKellar, J. Chem. Phys. **111**, 7321–7328 (1999). doi:10.1063/1.480055
[12] M. Rode, J. Sadlej, R. Moszynski, P.E.S. Wormer and A. van der Avoird, Chem. Phys. Lett. **314**, 326–332 (1999). doi:10.1016/S0009-2614(99)01168-9
[13] Y. Xu and W. Jäger, J. Chem. Phys. **111**, 5754–5756 (1999). doi:10.1063/1.479871
[14] K. Walker, C. Xia and A. McKellar, J. Chem. Phys. **113**, 6618–6623 (2000). doi:10.1063/1.1310607
[15] P.E.S. Wormer and A. van der Avoird, Chem. Rev. **100**, 4109–4144 (2000). doi:10.1021/cr990046e
[16] A.R.W. McKellar, J. Chem. Phys. **115**, 3571–3577 (2001). doi:10.1063/1.1387477
[17] T.B. Pedersen, B. Fernández and H. Koch, Chem. Phys. Lett. **334**, 419–423 (2001). doi:10.1016/S0009-2614(00)01328-2
[18] M. Rode, J. Sadlej, R. Moszynski, P.E. Wormer and A. van der Avoird, Chem. Phys. Lett. **334**, 424–425 (2001). doi:10.1016/S0009-2614(00)01329-4
[19] K. Walker and A. McKellar, J. Mol. Spectrosc. **208**, 209–212 (2001). doi:10.1006/jmsp.2001.8391
[20] T. Korona, R. Moszynski and B. Jeziorski, Mol. Phys. **100**, 1723–1734 (2002). doi:10.1080/00268970110105424
[21] J. Tang, A. McKellar, L. Surin, D.N. Fourzikov, B.S. Dumesh and G. Winnewisser, J. Mol. Spectrosc.**214**, 87–93 (2002). doi:10.1006/jmsp.2002.8579
[22] A.V. Burenin, Opt. Spectrosc. **95**, 192–200 (2003). doi:10.1134/1.1604424
[23] J. Fiser, T. Boublík and R. Polák, Mol. Phys. **101**, 3409–3418 (2003). doi:10.1080/0026897032000159378
[24] G.W.M. Vissers, P.E.S. Wormer and A. van der Avoird, Phys. Chem. Chem. Phys. **5**, 4767–4771 (2003). doi:10.1039/b309468e
[25] B.S. Dumesh, V.A. Panfilov, L.A. Surin, D.N. Furzikov and G. Winnewisser, JETP Lett. **80**, 98–102 (2004). doi:10.1134/1.1804217
[26] A. McKellar, J. Mol. Spectrosc. **226**, 190–195 (2004). doi:10.1016/j.jms.2004.04.007
[27] L.A. Surin, D.N. Fourzikov, B.S. Dumesh, G. Winnewisser, J. Tang and A.R.W. McKellar, J. Mol. Spectrosc. **223**, 132–137 (2004). doi:10.1016/j.jms.2003.10.009
[28] G.W.M. Vissers, A. Heßelmann, G. Jansen, P.E.S. Wormer and A. van der Avoird, J. Chem. Phys. **122**, 054306054306 (2005). doi:10.1063/1.1835262
[29] L. Surin, D.N. Fourzikov, T. Giesen, S. Schlemmer, G. Winnewisser, V. Panfilov, B.S. Dumesh, G. Vissers and A. van der Avoird, J. Chem. Phys. **125**, 094304094304 (2006). doi:10.1063/1.2345202
[30] L.A. Surin, D.N. Fourzikov, T.F. Giesen, S. Schlemmer, G. Winnewisser, V.A. Panfilov, B.S. Dumesh, G.W.M. Vissers and A. van der Avoird, J. Phys. Chem. A **111**, 12238–12247 (2007). doi:10.1021/jp0743471
[31] K.M.T. Yamada, J. Mol. Spectrosc. **254**, 87–93 (2009). doi:10.1016/j.jms.2009.01.007
[32] A. van der Avoird and L.A. Surin, J. Mol. Spectrosc. **259**, 60–61 (2010). doi:10.1016/j.jms.2009.11.002
[33] R. Dawes, X.-G. Wang and T. Carrington, J. Phys. Chem. A **117**, 7612–7630 (2013). doi:10.1021/jp404888d
[34] M. Rezaei, S. Sheybani-Deloui, N. Moazzen-Ahmadi, K.H. Michaelian and A.R.W. McKellar, J. Phys. Chem. A **117**, 9612–9620 (2013). doi:10.1021/jp312337v
[35] S.A. Ndengué, R. Dawes and F. Gatti, J. Phys. Chem. A **119**, 7712–7723 (2015). doi:10.1021/acs.jpca.5b01022

[36] P.R.P. Barreto, A.C.P. Cruz, R.L. Barreto, F. Palazzetti, A.F. Albernaz, A. Lombardi, G.S. Maciel and V. Aquilanti, J. Mol. Spectrosc. **337**, 163–177 (2017). doi:10.1016/j.jms.2017.05.009
[37] Z.-F. Sun, M.C. van Hemert, J. Loreau, A. van der Avoird, A.G. Suits and D.H. Parker, Science **369**, 307–309 (2020). doi:10.1126/science.aan2729
[38] A. Méry, V. Kumar, X. Fléchard, B. Gervais, S. Guillous, M. Lalande, J. Rangama, W. Wolff and A. Cassimi, Phys. Rev. A **103**, 042813042813 (2021). doi:10.1103/PhysRevA.103.042813.
[39] B.K. Oram, S. Sarkar, Monu and B. Bandyopadhyay, Comput. Theor. Chem. **1215**, 113849 (2022). doi:10.1016/j.comptc.2022.113849
[40] D. Bostan, B. Mandal, C. Joy, M. Żołtowski, F. Lique, J. Loreau, E. Quintas-Sánchez, A. Batista-Planas, R. Dawes and D. Babikov, Phys. Chem. Chem. Phys. **26**, 6627–6637 (2024). doi:10.1039/D3CP05369E
[41] C.J. Zhang, R.T. Zhang, S.C. Yan, L.P. Zou, S.F. Zhang, K. Hansen, P. Slavíček and X. Ma, J. Chem. Phys. **162**, 054302054302 (2025). doi:10.1063/5.0244051
[42] M.L. McKee, WIREs Comput. Mol. Sci. **1**, 943–951 (2011). doi:10.1002/wcms.v1.6
[43] A.G. Császár, C. Fábri and J. Sarka, WIREs Comput. Mol. Sci. **10**, e1432 (2019).
[44] D.A. Roth, L.A. Surin, B.S. Dumesh, G. Winnewisser and I. Pak, J. Chem. Phys. **113**, 3034–3038 (2000). doi:10.1063/1.1287141
[45] T.B. Adler, G. Knizia and H.-J. Werner, J. Chem. Phys. **127**, 221106221106 (2007). doi:10.1063/1.2817618
[46] S.F. Boys and F. Bernardi, Mol. Phys. **19**, 553–566 (1970). doi:10.1080/00268977000101561
[47] M. Kodrycka and K. Patkowski, J. Chem. Phys. **151**, 070901070901 (2019). doi:10.1063/1.5116151
[48] S. Simon, M. Duran and J.J. Dannenberg, J. Chem. Phys. **105**, 11024–11031 (1996). doi:10.1063/1.472902
[49] P. Hobza, O. Bludský and S. Suhai, Phys. Chem. Chem. Phys. **1**, 3073–3078 (1999). doi:10.1039/a902109d
[50] B. Paizs, P. Salvador, A.G. Császár, M. Duran and S. Suhai, J. Comp. Chem. **22**, 196–207 (2001). doi:10.1002/(ISSN)1096-987X
[51] W. Klopper and W. Kutzelnigg, Chem. Phys. Lett. **134**, 17–22 (1987). doi:10.1016/0009-2614(87)80005-2
[52] W. Klopper, F.R. Manby, S. Ten-No and E.F. Valeev, Int. Rev. Phys. Chem. **25**, 427–468 (2006). doi:10.1080/01442350600799921
[53] O. Marchetti and H.-J. Werner, Phys. Chem. Chem. Phys. **10**, 3400–3409 (2008). doi:10.1039/b804334e
[54] W. Kutzelnigg and W. Klopper, J. Chem. Phys. **94**, 1985–2001 (1991). doi:10.1063/1.459921
[55] L. Kong, F.A. Bischoff and E.F. Valeev, Chem. Rev. **112**, 75–107 (2011). doi:10.1021/cr200204r
[56] C. Hättig, W. Klopper, A. Köhn and D.P. Tew, Chem. Rev. **112**, 4–74 (2012). doi:10.1021/cr200168z
[57] T. Helgaker, W. Klopper, H. Koch and J. Noga, J. Chem. Phys. **106**, 9639–9646 (1997). doi:10.1063/1.473863
[58] G. Tarczay, A.G. Császár, W. Klopper, V. Szalay, W.D. Allen and H.F. Schaefer III, J. Chem. Phys. **110**, 11971–11981 (1999). doi:10.1063/1.479135
[59] T. Helgaker, P. Jorgensen and J. Olsen, *Molecular Electronic-Structure Theory* (Wiley, New York, 2000).
[60] W.D. Allen, A.L.L. East and A.G. Császár, in *Structures and Conformations of Nonrigid Molecules*. (1993), pp. 343–373.
[61] A.G. Császár, W.D. Allen and H.F. Schaefer III, J. Chem. Phys. **108**, 9751–9764 (1998). doi:10.1063/1.476449
[62] K. Szalewicz, WIREs Comput. Mol. Sci. **2**, 254–272 (2012). doi:10.1002/wcms.v2.2
[63] K. Patkowski, WIREs Comput. Mol. Sci. **10**, e1452 (2019). doi:10.1002/wcms.1452
[64] C. Møller and M.S. Plesset, Phys. Rev. **46**, 618–622 (1934). doi:10.1103/PhysRev.46.618
[65] K. Raghavachari, G.W. Trucks, J.A. Pople and M. Head-Gordon, Chem. Phys. Lett. **157**, 479–483 (1989). doi:10.1016/S0009-2614(89)87395-6
[66] W.D. Allen and A.G. Császár, J. Chem. Phys. **98**, 2983–3015 (1993). doi:10.1063/1.464127
[67] R. Tóbiás, P. Árendás and A.G. Császár, J. Chem. Theor. Comput. **18**, 1788–1798 (2022). doi:10.1021/acs.jctc.1c01148
[68] I.M.B. Nielsen, W.D. Allen, A.G. Császár and H.F. Schaefer, J. Chem. Phys. **107**, 1195–1211 (1997). doi:10.1063/1.474612
[69] T.J. Lee and P.R. Taylor, Int. J. Quant. Chem. Symp. **23**, 199–207 (1989).
[70] T.H. Dunning, Jr., J. Chem. Phys. **90**, 1007–1023 (1989). doi:10.1063/1.456153
[71] G. Tasi and A.G. Császár, Chem. Phys. Lett. **438**, 139–143 (2007). doi:10.1016/j.cplett.2007.02.056
[72] A. Halkier, T. Helgaker, P. Jørgensen, W. Klopper and J. Olsen, Chem. Phys. Lett. **302**, 437–446 (1999). doi:10.1016/S0009-2614(99)00179-7
[73] R. Tóbiás, C. Fábri, M. Bosquez, M. Kodrycka, K. Patkowski and A.G. Császár, Commun. Chem. **8**, 339 (2025). doi:10.1038/s42004-025-01716-7
[74] R.D. Cowan and D.C. Griffin, J. Opt. Soc. Am. **66**, 1010–1014 (1976). doi:10.1364/JOSA.66.001010
[75] G. Tarczay, A.G. Császár, W. Klopper and H.M. Quiney, Mol. Phys. **99**, 1769–1794 (2001). doi:10.1080/00268970110073907
[76] N.C. Handy, Y. Yamaguchi and H.F. Schaefer III, J. Chem. Phys. **84**, 4481–4484 (1986). doi:10.1063/1.450020
[77] E.F. Valeev and C.D. Sherrill, J. Chem. Phys. **118**, 3921–3927 (2003). doi:10.1063/1.1540626
[78] D.G.A. Smith, L.A. Burns, A.C. Simmonett, R.M. Parrish, M.C. Schieber, R. Galvelis, P. Kraus, H. Kruse, R. Di Remigio, A. Alenaizan, A.M. James, S. Lehtola, J.P. Misiewicz, M. Scheurer, R.A. Shaw, J.B. Schriber, Y. Xie, Z.L. Glick, D.A. Sirianni, J.S. O'Brien, J.M. Waldrop, A. Kumar, E.G. Hohenstein, B.P. Pritchard, B.R. Brooks, H.F. Schaefer, A.Y. Sokolov, K. Patkowski, A.E. DePrince, U. Bozkaya, R.A. King, F.A. Evangelista, J.M. Turney, T.D. Crawford and C.D. Sherrill, J. Chem. Phys. **152**, 184108184108 (2020). doi:10.1063/5.0006002
[79] T.M. Parker, L.A. Burns, R.M. Parrish, A.G. Ryno and C.D. Sherrill, J. Chem. Phys. **140**, 094106094106 (2014). doi:10.1063/1.4867135
[80] E.G. Hohenstein and C.D. Sherrill, WIREs Comput. Mol. Sci. **2**, 304–326 (2012). doi:10.1002/wcms.v2.2
[81] S. Rybak, B. Jeziorski and K. Szalewicz, J. Chem. Phys. **95**, 6576–6601 (1991). doi:10.1063/1.461528

[82] H.L. Williams, K. Szalewicz, R. Moszynski and B. Jeziorski, J. Chem. Phys. **103**, 4586–4599 (1995). doi:10.1063/1.470646

[83] A. Heßelmann, G. Jansen and M. Schütz, J. Chem. Phys. **122**, 014103014103 (2004). doi:10.1063/1.1824898

[84] A.J. Misquitta, B. Jeziorski and K. Szalewicz, Phys. Rev. Lett. **91**, 033201033201 (2003). doi:10.1103/PhysRevLett.91.033201

[85] A.J. Misquitta, R. Podeszwa, B. Jeziorski and K. Szalewicz, J. Chem. Phys. **123**, 214103214103 (2005). doi:10.1063/1.2135288

[86] C. Adamo and V. Barone, J. Chem. Phys. **110**, 6158–6170 (1999). doi:10.1063/1.478522

[87] T. Korona, Mol. Phys. **111**, 3705–3715 (2013). doi:10.1080/00268976.2012.746478

[88] D.A. Matthews, L. Cheng, M.E. Harding, F. Lipparini, S. Stopkowicz, T.-C. Jagau, P.G. Szalay, J. Gauss and J.F. Stanton, J. Chem. Phys. **152**, 214108214108 (2020). doi:10.1063/5.0004837

[89] M.J. Frisch, G.W. Trucks, H.B. Schlegel, G.E. Scuseria, M.A. Robb, J.R. Cheeseman, G. Scalmani, V. Barone, G.A. Petersson, H. Nakatsuji, X. Li, M. Caricato, A.V. Marenich, J. Bloino, B.G. Janesko, R. Gomperts, B. Mennucci, H.P. Hratchian, J.V. Ortiz, A.F. Izmaylov, J.L. Sonnenberg, D. Williams-Young, F. Ding, F. Lipparini, F. Egidi, J. Goings, B. Peng, A. Petrone, T. Henderson, D. Ranasinghe, V.G. Zakrzewski, J. Gao, N. Rega, G. Zheng, W. Liang, M. Hada, M. Ehara, K. Toyota, R. Fukuda, J. Hasegawa, M. Ishida, T. Nakajima, Y. Honda, O. Kitao, H. Nakai, T. Vreven, K. Throssell, J.A. Montgomery, Jr., J.E. Peralta, F. Ogliaro, M.J. Bearpark, J.J. Heyd, E.N. Brothers, K.N. Kudin, V.N. Staroverov, T.A. Keith, R. Kobayashi, J. Normand, K. Raghavachari, A.P. Rendell, J.C. Burant, S.S. Iyengar, J. Tomasi, M. Cossi, J.M. Millam, M. Klene, C. Adamo, R. Cammi, J.W. Ochterski, R.L. Martin, K. Morokuma, O. Farkas, J.B. Foresman and D.J. Fox, *Gaussian 16 Revision B.01* (Gaussian Inc, Wallingford CT, 2016).

[90] *MOLPRO website, last accessed on February 12, 2026.*

[91] *MRCC website, last accessed on February 12, 2026.*

[92] D. Mester, P.R. Nagy, J. Csóka, L. Gyevi-Nagy, P.B. Szabó, R.A. Horváth, K. Petrov, B. Hégely, B. Ladóczki, G. Samu, B.D. Lörincz and M. Kállay, J. Phys. Chem. A **129**, 2086–2107 (2025). doi:10.1021/acs.jpca.4c07807

[93] G. Rauhut, J. Chem. Phys. **121**, 9313–9322 (2004). doi:10.1063/1.1804174

[94] B. Ziegler and G. Rauhut, J. Chem. Phys. **149**, 164110164110 (2018). doi:10.1063/1.5047912

[95] A.G. Császár, C. Fábri, T. Szidarovszky, E. Mátyus, T. Furtenbacher and G. Czakó, Phys. Chem. Chem. Phys. **14**, 1085–1106 (2012). doi:10.1039/C1CP21830A

[96] J. Baker, J. Comp. Chem. **7**, 385–395 (1986). doi:10.1002/jcc.v7:4

[97] J. Baker and F. Chan, J. Comp. Chem. **17**, 888–904 (1996). doi:10.1002/(ISSN)1096-987X

[98] A.R. Dixon, T. Xue and A. Sanov, Angew. Chem. Int. Ed. **54**, 8764–8767 (2015). doi:10.1002/anie.v54.30

[99] D. Davis and Y. Sajeev, J. Chem. Phys. **146**, 081101081101 (2017). doi:10.1063/1.4976969

[100] J. Mato, D. Poole and M.S. Gordon, J. Phys. Chem. A **124**, 8209–8222 (2020). doi:10.1021/acs.jpca.0c06107

[101] A.G. Császár, W.D. Allen, Y. Yamaguchi and H.F. Schaefer, III, in *Computational Molecular Spectroscopy*. (2000), pp. 15–68.

[102] A.G. Császár, G. Tarczay, M.L. Leininger, O.L. Polyansky, J. Tennyson and W.D. Allen, in *Spectroscopy from Space*. (2001), pp. 317–339.

[103] J. Demaison and A.G. Császár, J. Mol. Struct. **1023**, 7–14 (2012). doi:10.1016/j.molstruc.2012.01.030

[104] J. Demaison, N. Vogt, Y. Jin, R.T. Saragi, M. Juanes and A. Lesarri, J. Chem. Phys. **154**, 194302194302 (2021). doi:10.1063/5.0048603

[105] W.D. Allen and A.G. Császár, in *Equilibrium Molecular Structures*. (CRC Press, Boca Raton, 2011), pp. 1–28.

[106] E. Tiemann, H. Arnst, W.U. Stieda, T. Törring and J. Hoeft, Chem. Phys. **67**, 133–138 (1982). doi:10.1016/0301-0104(82)85027-1

[107] A.G. Császár, M. Leininger and V. Szalay, J. Chem. Phys. **118**, 10631–10642 (2003). doi:10.1063/1.1573180

[108] G. Czakó, E. Mátyus, A.C. Simmonett, A.G. Császár, H.F. Schaefer and W.D. Allen, J. Chem. Theor. Comput. **4**, 1220–1229 (2008). doi:10.1021/ct800082r

[109] H.M. Jaeger, H.F. Schaefer, J. Demaison, A.G. Császár and W.D. Allen, J. Chem. Theor. Comput. **6**, 3066–3078 (2010). doi:10.1021/ct1000236

[110] R. Tóbiás, A.G. Császár, L. Gyevi-Nagy and G. Tasi, J. Comp. Chem. **39**, 424–437 (2018). doi:10.1002/jcc.v39.8

[111] J. Garcia, R. Podeszwa and K. Szalewicz, J. Chem. Phys. **152**, 184109184109 (2020). doi:10.1063/5.0005093

[112] J.S. Muenter, J. Mol. Spectrosc. **55**, 490–491 (1975). doi:10.1016/0022-2852(75)90287-8

[113] G. Frenking, C. Loschen, A. Krapp, S. Fau and S.H. Strauss, J. Comp. Chem. **28**, 117–126 (2007). doi:10.1002/jcc.v28:1

[114] G.E. Scuseria, M.D. Miller, F. Jensen and J. Geertsen, J. Chem. Phys. **94**, 6660–6663 (1991). doi:10.1063/1.460293

[115] O. Christiansen, C. Hättig and J. Gauss, J. Chem. Phys. **109**, 4745–4757 (1998). doi:10.1063/1.477086

[116] T. Korona, J. Chem. Phys. **128**, 224104224104 (2008). doi:10.1063/1.2933312